Multiheterogeneous AUV Swarm Technology Exemplified by the MAUS Project: Cooperation, Mission Planning and Hybrid Communication

Sabah Badri-Hoeher, Thomas Wilts, Lukas Schaefer, Jonni Westphalen, Julian Winkler, Cedric Isokeit, Andrej Harlakin, Maurice Hott, Julius Maximilian Placzek, Stefan Marx, Martin Volz, Erik Maehle, *Member, IEEE*, and Peter Adam Hoeher, *Fellow, IEEE*

***Abstract*—The mobile autonomous underwater system (MAUS) aims to create next-generation vehicles, focusing on improved intelligence, mission operations, and application scenarios. Accordingly, two types of autonomous underwater vehicles (AUVs) have been developed to operate and collaborate in various applications. The first AUV, named "Hansel," has hovering capabilities and is tailored to tasks, such as object inspection and detection. The second AUV, called "Gretel," has going capabilities and is suitable for tasks, such as seafloor mapping. The two AUV types are equipped with different sensors, allowing them to perform distinct tasks simultaneously as a team. The going AUV has a robust navigation system that includes an inertial navigation system, an ultra-short baseline unit, and a Doppler velocity log for dead reckoning. In contrast, the hovering AUV only has a low-cost micro-electro-mechanical system. Gretel's navigation unit improves Hansel's navigation, along with data transfer between the vehicles. The AUVs rely on a hybrid communication system that integrates acoustic, inductive, and optical links to combine the strengths of each technology. To accomplish their individual goals, the AUVs participate in joint mission planning, utilizing a variety of sensors and tasks that are specific to each AUV. This approach is commonly referred to as multiheterogeneous AUV swarm technology. The multiheterogeneous concept developed in the MAUS project was experimentally validated in Kiel Fjord, located in the southwest Baltic Sea, and in La Spezia, Mediterranean Sea.**

***Index Terms*—Autonomous underwater vehicles (AUVs), autonomy, communications technology, computational intelligence, sensors, swarm navigation, underwater communication, underwater swarm robotics.**

Received 17 February 2023; revised 31 January 2024; accepted 14 July 2024. Date of publication 5 November 2024; date of current version 14 January 2025. This work was supported by the MAUS through EU.SH project under Grant LPW-E/1.2.2. *(Corresponding author: Sabah Badri-Hoeher.)*

Associate Editor: A. Munafo.

Sabah Badri-Hoeher, Thomas Wilts, Lukas Schaefer, Jonni Westphalen, and Julian Winkler are with the Faculty of Computer Science and Electrical Engineering, University of Applied Sciences Kiel, D-24148 Kiel, Germany (e-mail: sabah.badri-hoeher@fh-kiel.de; thomas.wilts@fh-kiel.de; lukasschaefer.ger@gmail.com; jonny.westphalen@gmail.com; julian.winkler@web.de).

Cedric Isokeit and Erik Maehle are with the Institute of Computer Engineering, Luebeck University, D-23562 Luebeck, Germany (e-mail: cedrik.isokeit@gmx.de; maehle@iti.uni-luebeck.de).

Andrej Harlakin, Maurice Hott, Julius Maximilian Placzek, and Peter Adam Hoeher are with the Faculty of Engineering, Kiel University, D-24143 Kiel, Germany (e-mail: anha@tf.uni-kiel.de; maho@tf.uni-kiel.de; jmpl@tf.uni-kiel.de; ph@tf.uni-kiel.de).

Stefan Marx is with the SubCtech GmbH, D-24145 Kiel, Germany (e-mail: marx@subctech.com).

Martin Volz is with the Emma Technologies GmbH, D-24251 Osdorf, Germany (e-mail: volz@emma-technologies.com).

Digital Object Identifier 10.1109/JOE.2024.3451241

Acronyms

ASK	Amplitude shift keying.
AUV	Autonomous underwater vehicle.
CI	Continuous integration.
CLC	Creeping line search, coordinated.
CNC	Computerized numerical control.
CPU	Central processing unit.
DC	Direct current.
DSC	Dual side control.
DSSS	Direct-sequence spread spectrum.
DSP	Digital signal processing.
DVL	Doppler velocity log.
ESC	Electronic speed controller.
FH-FSK	Frequency-hopping frequency shift keying.
FOG	Fiber optic gyroscope.
FSK	Frequency shift keying.
GUI	Graphical user interface.
HAT	Hardware attached on top.
IDE	Integrated development environment.
IM/DD	Intensity modulation and direct detection.
INS	Inertial navigation system.
IPT	Inductive power transfer.
LED	Light emitting diode.
MAUS	Mobile autonomous underwater system.
MEMS	Micro-electro-mechanical system.
miniCT	Conductivity and temperature sensor.
miniSVS	Sound velocity sensor.
MFSK	M-ary frequency shift keying.
MOSFET	Metal-oxide-semiconductor field-effect transistor.
MRFSK	Multiresonant frequency shift keying.
MPH	Main pressure hull.
OFDM	Orthogonal frequency-division multiplexing.
OOI	Object of interest.
OOK	ON–OFF keying.
OpAmp	Operational amplifier.
PCB	Printed circuit board.
PD	Photodiode.
POM	Polyoxymethylene.

PSK	Phase shift keying.
ROB	Reserve of buoyancy.
ROS	Robot operating system.
SDR	Software-defined radio.
SNR	Signal-to-noise ratio.
UART	Universal asynchronous receiver transmitter.
UAWC	Underwater acoustic wireless communication.
UMWC	Underwater magnetic wireless communication.
UOWC	Underwater optical wireless communications.
USB	Universal serial bus.
USBL	Ultra-short baseline.
ZCS	Zero current switching.
ZVS	Zero voltage switching.

I. Introduction

THE world's seas and oceans were once used solely as waterways or as a source of food. But with the accumulation of environmental disasters and the search for new energy sources, people have begun to intensively research and explore the oceans. In shallow as well as in deep waters, many exploration tasks can only be accomplished through the use of underwater robots. Underwater robots can be classified as remotely operated vehicles and AUVs. The global AUV market is experiencing significant growth, expanding to fulfill a diverse range of underwater applications [1], [2], [3], [4]. AUV missions are numerous and diverse, and can be divided in scientific and environmental, commercial, and military fields. Examples of scientific and environmental applications are oceanography, environmental observation, and habitat monitoring and survey. Commercial applications include monitoring and inspection of gas and oil pipelines, harbor areas, and offshore wind parks. In the naval sector, the tasks include reconnaissance and detection of ammunition. If only a single AUV is deployed, a long mission duration may be necessary, especially if there are multiple tasks to be accomplished. This often involves large and heavy vehicle types that require sophisticated infrastructure and can therefore be time-consuming and costly. In the worst case and with increasing complexity of a mission, some tasks remain unsolvable with a single AUV.

Nowadays, swarms of small AUVs are becoming more and more important and mature. The swarm concept is inspired by social insects, birds, or schools of fish. Distributed self-organizing systems of autonomous robots can cooperate to achieve global or local goals if communication links can be established between the agents. Robotic swarms offer several advantages. In general, the agents are of smaller size compared to classical robots. Ideally, they have few and simple sensors that benefit from communication. In this case, the success of a mission is due to the cooperation of all members to accomplish tasks that they cannot solve individually. In a robotic swarm, the collective action of the robots results from local interactions among themselves as well as with their operating environment. In addition, the swarm structure enables parallelization, which not only reduces deployment time and improves robustness, but also allows for efficient utilization of resources, making it highly scalable. Underwater swarm robotics can be profitably applied in all the scientific and environmental, commercial, and military fields already mentioned, but beyond solving classical tasks it can generate supplementary benefits.

A. Related Work

1) Related Academic Work: The design of robotic swarms is guided by principles of swarm intelligence [5], [6]. These principles promote the realization of systems that are fault-tolerant, scalable, and flexibly applicable. Initially, swarm research focused on the study and validation of biological research [7], [8]. Early collaborations between robotics researchers and biologists helped launching swarm robotics research, which has since become a research field in its own right. Over the years, the focus of swarm robotics has evolved: from a biologically inspired field of robotics, swarm robotics is increasingly becoming an engineering field focused on developing tools and methods to solve real-world problems [9].

On the subject of underwater swarm robotics, extensive research has already been published. These cover both algorithmic design, particularly regarding coordination control [10], [11], [12], as well as vehicle design [13], [14], [15], [16], [17]. Concerning swarm navigation, theoretical foundations are well established [18], [19]. In addition, overview papers have been published, see for example [20] and [21]. Still, design considerations are not yet mature [22], [23], [24], [25] and many challenges remain [26]. Among the objectives of our contribution is to provide specific design hints for a team/swarm of AUVs that benefit from different sensor technology.

Reliable communication is one of the key issues in swarm robotics. Considering that the underwater channel is a harsh environment on the one hand, but on the other hand distances between the nodes can be adjusted (known as coordination, consensus control, flocking, etc.), this project focuses on acoustic, magnetic and optical communication—depending on the situation. Our UMWC modem is based on a novel approach, where the receiver coil of a classical magneto-inductive communication system [27], [28], [29], [30] has been replaced by a magnetic detector, which is based on one or several high-sensitivity low-noise wideband magnetic field sensors. Related work has independently been published in [31], where the emphasis is on diver communication employing a speech codec, and in [32], where magnetic field detectors based on the giant magneto-impedance effect are studied for communication purposes, motivated by our original work in [33] and [34]. Magnetic communication is suitable for harsh environments where optical communication fails, such as in turbid waters. Range and bandwidth can be easily traded off against each other.

UOWC has attracted considerable interest in recent years because the achievable data rates exceed those of acoustic and magnetic communications when there is sufficient visibility between the transmitter and receiver. Numerous optical modems with different specifications have been developed. A comprehensive overview can be found in [35], [36], [37], [38], and [39]. In recent times, related research focused on improved coverage as well as on higher data rates. Regarding coverage, hybrid approaches, such as optical-acoustic sensor networks

have been investigated [40]. It was confirmed that UOWC can complement acoustic modems with high-rate communication at short to medium ranges. Among the objectives of our optical modem design is to avoid a classic pressure housing by using the pressure-neutral casting technique elaborated in [39] to save volume, weight, and cost. With ∼10 W power, data rates on the order of 1–10 Mbps are realistic for distances of tens of meters in clean seawater. To achieve data rates in the Gbps range, micro LED arrays have proven suitable in the meter range [41].

2) Related Research Projects: Nowadays, many underwater research projects are considering the integration of underwater robots for various scientific tasks. For example, the *autonomous robotic sea-floor infrastructure for bentho-pelagic monitoring* project, involving six European marine research institutes, aims to provide continuous online ocean monitoring. Static underwater systems are combined with mobile robots for environmental monitoring. The mobile robot will improve marine monitoring and will be used for scientific purposes. The *offshore robotics for the certification of assets* project, set up by the U.K. government, aims to combine robotic systems and artificial intelligence to redefine asset integrity management for the offshore energy sector. A third example is the *integrated technologies longterm deployment of robotic underwater platforms* project, which is cofunded by the EU together with other partners. The project aims to ensure that AUVs can be deployed for extended time periods to perform their assigned tasks without external interruption. To achieve this goal, the partners are focusing on underwater contactless power transmission and wireless communications. However, such science projects rarely publish details about AUV swarm construction.

B. Contribution

The EU.SH project "MAUS," funded by the EU and the federal state of SH, targets the hardware and software design, communication strategy, and route planning of an AUV swarm. The main contributions of this collaborative project are reported next and can be summarized as follows.

1) The AUV swarm concept utilizes collective actions and assigns different tasks and sensors to two different AUV types, resulting in optimized mission performance. Among other things, a guiding system for an equipment carrier without expensive navigation sensors is being implemented in the MAUS project. This allows one AUV to continuously scan for points of interest while the other can be guided to these locations by acoustic communication. This optimizes the use of resources.
2) Innovative and artificial intelligence (AI)-based algorithms are employed in mission planning and execution, significantly increasing the AUV swarm's autonomy. In order to plan the paths and the mission of the AUVs, computational geometry methods are used to achieve a result quickly and efficiently even for the limited hardware resources of an AUV. This ensures a deterministic result and training is not necessary.
3) For the first time, inductive, optical, and acoustic underwater communication technologies are efficiently combined in a hybrid modem to enhance the ability of swarm-based communication. A corresponding task scheduling procedure is suggested and experimentally verified.

The developed AUVs are highly modular, small, lightweight, low cost, and have a long time of operation. The hardware components of the AUVs are easily replicable, which simplifies the process of duplicating the vehicles. With this method, AUVs can be easily scaled up to form larger swarms for more challenging missions. Moreover, the modularity of the AUV components allows for addition of new functionalities as needed.

C. Organization

The rest of this article is organized as follows. In Section II, a system overview is given covering the general system description, mechanical design and construction aspects, electrical and sensor integration, as well as the software framework and an innovative battery system with inductive energy transmission. Section III presents the data modems and communication strategies developed within the MAUS project. The swarm navigation and autonomy concept is introduced in Section IV. Section V includes the experimental results and field trials. Finally, Section VI concludes this article.

II. System Overview and Description

A. General System Description

The collaborative MAUS project, involving academic institutions and manufacturers, developed and built two different types of AUVs as prototypes. Both AUV types are modular, innovative, and suitable for solving different tasks. Among the applications are the optical and acoustic mapping of offshore structures and the seafloor as well as the photic zone (Gretel), and the measurement of various parameters of the water column with different chemical and physical sensors (Hansel). By nature, AUV projects, such as this one are multidisciplinary. The focus of this section is on mechanical design and construction, integration of electrical components and sensors, description of the software framework, and reporting on the innovative battery system and inductive energy transmission.

B. Mechanical Design and Construction

The mechanical structure of the two AUV types was individually designed according to the tasks that each AUV has to perform. Both vehicles are designed for a maximum depth of 200 m.

The hovering AUV Hansel is 1292 mm long, 452 mm high, 550 mm wide, and weights 46 kg in air. Its structure, depicted in Fig. 1, consists of two longitudinal frames connected by two transverse ribs. All pressure bodies, two lithium-ion battery modules, and thrusters are attached to this structure. To cope with the corrosion in the water and the forces acting on the vehicle, the supporting elements are made of POM. The role of the Hansel vehicle as a hover-capable AUV for inspection tasks leads to significant differences in the equipment, compared to Gretel. Hansel must have sufficient control authority to compensate for disturbances, such as currents. Therefore, the vehicle is equipped with seven thrusters of type T200 from Blue Robotics, which are allocated in all three spatial directions. This configuration uses

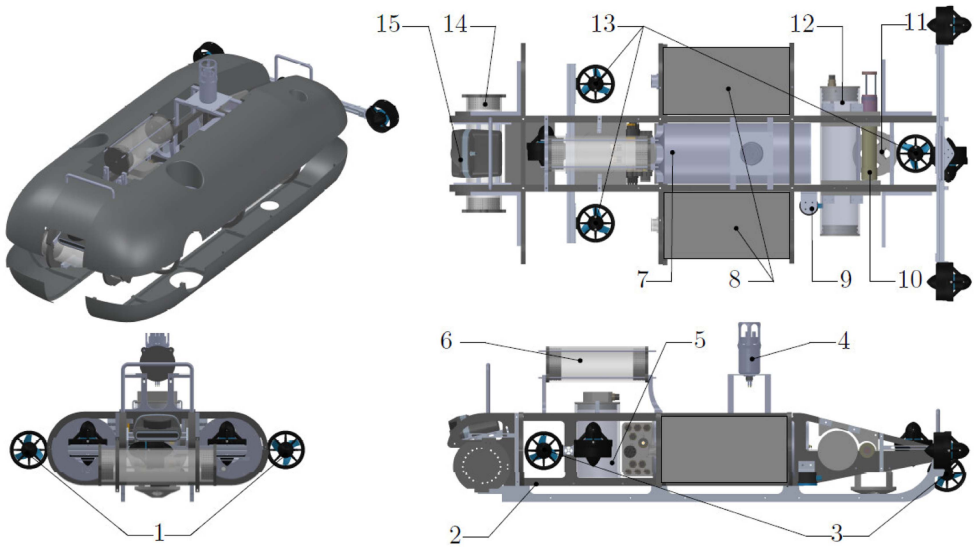

Fig. 1. Technical drawing of AUV Hansel. This AUV has hovering capabilities. The left upper image shows its housing and buoyancy foam. The main components are: (1) horizontal thruster, (2) camera flash, (3) traverse thruster, (4) USBL, (5) 4 K camera, (6) antenna, (7) MPH, (8) batteries, (9) altimeter, (10) conductivity and temperature sensor, (11) optical transceiver, (12) optical and magnetic communication pressure hull, (13) vertical thruster, (14) stereo camera, and (15) forward-looking sonar.

a differential drive for simple position control of the vehicle in the horizontal plane, while three vertical thrusters are used for depth control. These are controlled by, which receive the control instructions from the main computer, an UpXtreme. Both components are located in the MPH, in the center of the vehicle between the two batteries. Hansel is equipped with an M1200D Oculus-type imaging sonar from Blueprint Subsea in the bow, serving as a forward-looking sonar. Located underneath is a stereo camera system, an in-house development, to provide stereo imaging. In addition to camera images of objects in front of the vehicle, it can also be used to calculate depth information from the overlap of the two images. Directly behind is a high-resolution camera that, together with a flash, takes pictures of the seabed. In the rear part of the vehicle, directly behind the MPH, is the pressure body for the optical and magnetic communication systems. Next to it, a miniCT from Valeport and a ping sonar altimeter from Blue Robotics is placed. With the data from the altimeter and miniCT, the vehicle can either maintain a predefined diving depth or a fixed distance above the seabed. At the top of the vehicle, above the MPH, an antenna pressure body and an USBL transceiver are positioned. In addition to a Wi-Fi antenna and a GPS receiver, the antenna pressure body contains an emergency stop switch with a reed contact that is actuated from the outside by inserting a magnetic pin. Hansel utilizes the USBL system for relative positioning to Gretel. Electrical connections between the components are realized via connectors from Subconn, which can be plugged in even when wet.

The going AUV Gretel in Fig. 2 is 1230 mm long, 380 mm high, 570 mm wide, and weights 50 kg in air. The basic shape is determined by two longitudinal frames onto which three ribs are bolted. A rail is mounted under each of the two frame elements to protect against grounding. Above the frames the buoyancy foam is fixed, which allows a positive residual buoyancy of 1–2 kg. At the rear, there is a 20×20 MK aluminum profile that connects the frames together. For seawater resistance, aluminum alloy with magnesium is used. Propulsion and rudder action are implemented by a total of six T200 thrusters from Blue Robotics. Four thrusters are attached horizontally to the aft MK aluminum profile and provide thrust and enable steering in the horizontal plane. Two thrusters are attached vertically to the front rib to implement depth control. The MPH, the two lithium-ion battery modules provided by SubCtech, the side-scan sonar from BluePrint SubSea, and the antenna are located in the center of the vehicle. The batteries are encapsulated in a titanium pressure hull and are held in place by two ribs. The energy capacity is 1.4 kWh each at 21.6 V and 66 A. The side-scan sonar is also attached to the ribs at an angle of 15°. The MPH is made of POM and is located between the two batteries. In addition to the MPH, the pressure bodies for the INS and the side-scan control are also made of POM. Both are mounted vertically in front of and behind the MPH. The rear third of the AUV also contains a pressure hull for the magnetic and optical communication control as well as a miniSVS from Valeport. Both are mounted horizontally across the frame to save space. Above this, integrated in the foam, is the coil for magnetic communication. In the front third of the AUV is a forward looking sonar from BluePrint SubSea, a DVL from Nortek, and above the INS pressure hull, the transmitter and receiver for optical communications. All subsea electrical connectors were supplied by SubConn. The hydrodynamic shape is provided by a hull that is attached to the vehicle.

Stability considerations for AUVs diving with active propulsion elements differ significantly from surface ships and conventional submarines that use ballast tanks to control buoyancy weight. In all vessels, the ROB plays an important role in stability and safety. ROB is defined as the enclosed volume above the waterline when the weight of the vehicle is equal to the weight of water displaced by its volume. In contrast, all submersibles need to meet stability conditions in both underwater and surface operations for safe operation. Stability conditions have been

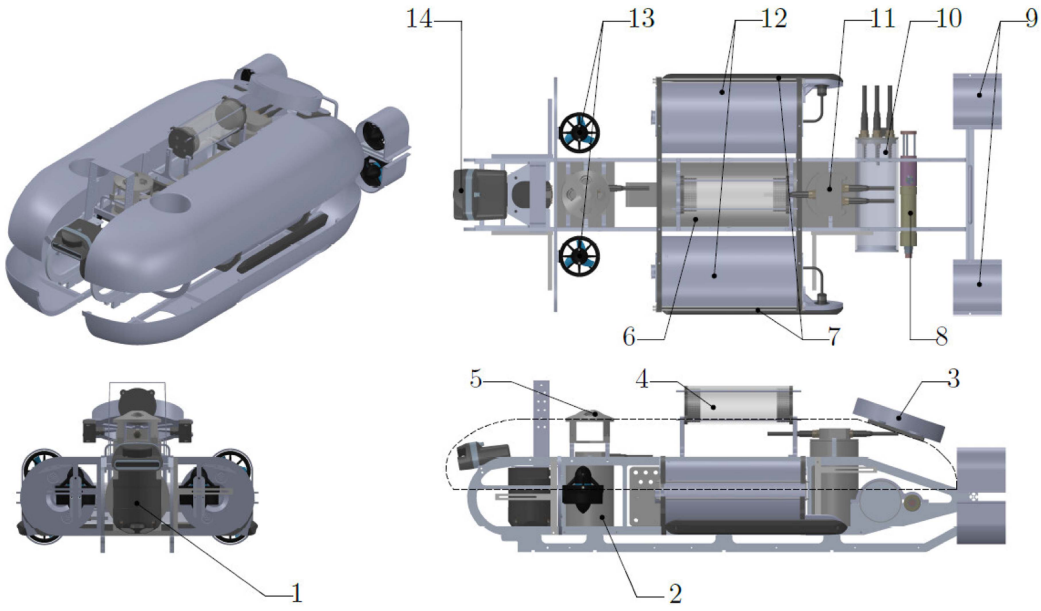

Fig. 2. Technical drawing of AUV Gretel. Gretel is a going AUV suitable for seafloor mapping and related applications. The left upper image shows its housing and buoyancy foam. The main components are: (1) DVL, (2) INS, (3) magnetic transmitter coil (transparent in top view), (4) antenna, (5) optical transceiver, (6) MPH, (7) side-scan sonar transducer, (8) sound velocity sensor, (9) horizontal thrusters, (10) optical and magnetic communication pressure hull, (11) side-scan sonar pressure hull, (12) batteries, (13) vertical thrusters, and (14) forward-looking sonar.

addressed through a thorough design process that is beyond the scope of this article.

C. Electrical and Sensors Integration

The essential components of the MAUS AUVs are shown in Figs. 3 and 4. A well-considered implementation of such components in terms of alignment and operational stability is mandatory. The heart of the AUVs is the smart power board that provides energy to each electrical device, monitors their currents, and switches each socket. All of these logical interactions are managed by a microcontroller that communicates with the main computer via RS-232. It is capable of providing a battery voltage of 24 V, as well as 12 and 5 V through multiple step-down converters. This fits most supply voltage requirements for underwater-specific hardware and consumer devices. The current per switch is limited to 25 A, and each switch can be set by external UART commands. Exceptional operating values are sent to the main computer for fault detection and situational awareness. A deeper look into power management is given in Section II-E. A compact but powerful single board quad-core computer serves as main processing unit. It collects all sensor data, processes them, and controls the AUV as explained in Section II-D. Besides several USB connections, it has a 6-port Ethernet extension for sensor and tether connections. The disadvantage of most single-board computers is the lack of RS-232 connections, as required by several sensor devices. Hence, a sensor HAT board collects all RS-232-based communication and forwards it as a serial stream to the main computer. Furthermore, the sensor HAT reports hull faults using its on-board temperature and water ingress sensors. In addition, all ESC commands are passed by the sensor HAT via RS-232 or interintegrated circuit interfacing. All these electrical components are thermally coupled with an aluminum backplate that dissipates heat through the aluminum hull cover. Supplementary cooling fans and efficient spatial alignment of each component prevent hot spots around the and CPU. The electrical wiring is matched to the required length to reduce heat loss and electromagnetic disturbances. In the following sections, each sensor and its purpose are explained.

1) Navigational Sensors: Since the MAUS AUVs are supposed to last under water for at least 12 h, the choice and integration of the navigational sensors is crucial. Further, the MAUS concept requires a steady communication and localization between the vehicles. Therefore, an USBL system as well as an acoustic modem is attached to each vehicle. The range of the USBL links is limited to 1.5 km. Since the rate for location and information exchange is low in comparison to electromagnetic systems, both AUVs aid their navigation using for instance a DVL or accelerometers. Gretel's DVL is suited for depths up to 1000 m and is capable to measure the velocity above ground for up to 75 m at an 8-Hz update rate. To capture the alignment, an INS including a FOG is used. The advantages of over magnetic compasses are the robustness against electromagnetic disturbances and high accuracy that is mandatory for a precise navigation. On the other hand, require an initial north seeking phase and suffer from a random walk-like drift. The actual position of the AUV is calculated by feeding the speed measured by the DVL and the acceleration and heading given by the INS into an error-state Kalman filter [42].

Since Hansel is supposed to navigate relative to Gretel via USBL, accelerometers are used to estimate the motion between acoustic updates. In certain modes its navigation is aided by sonar-based positioning toward, as explained in detail in Section IV. A simple single-beam altimeter with a maximum range of 50 m secures operational height above ground. The

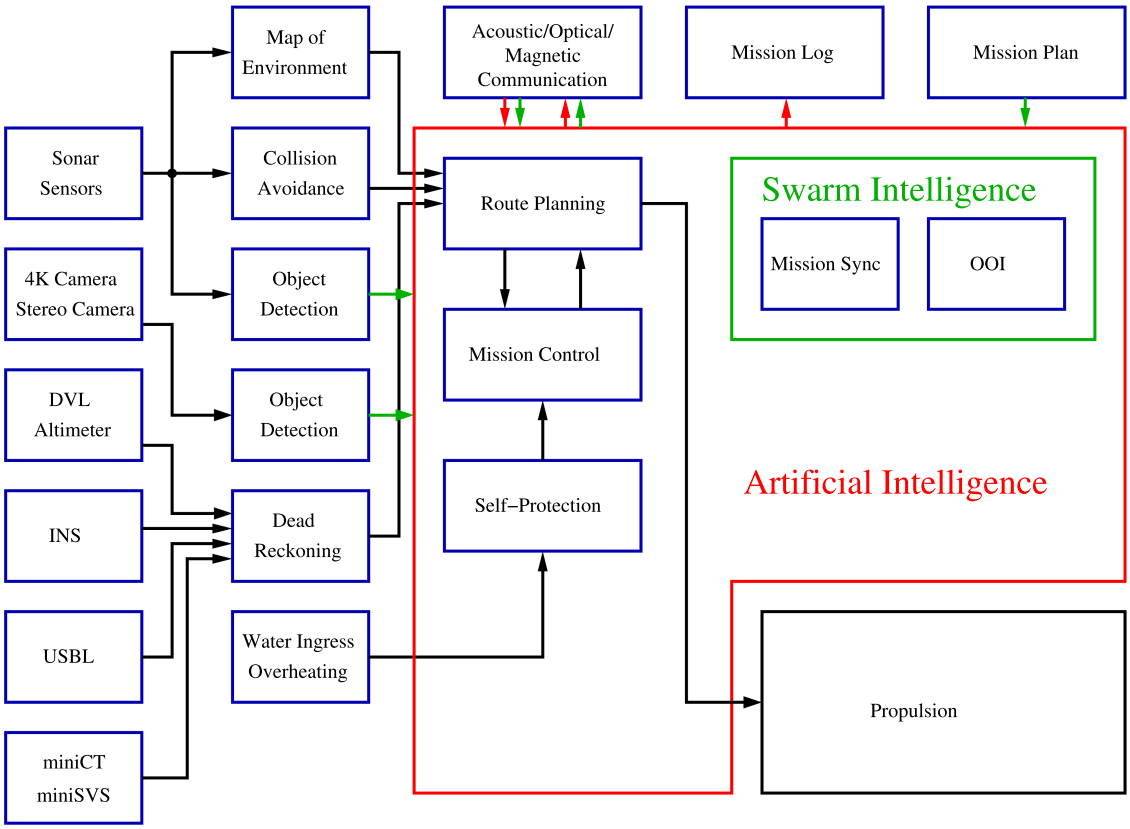

Fig. 3. Sensors and software modules of the AUVs are shown as block diagram. Depending on the configuration, only a subset of modules is active. Artificial intelligence is applied in the following tasks: route planning, mission control, self-protection, and swarm intelligence.

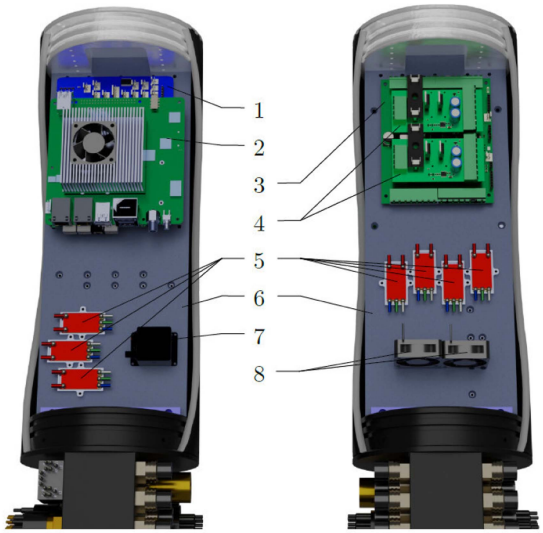

Fig. 4. Integration of internal hardware. The main computer (2) with the Ethernet extension uses the sensor HAT (1) for synchronized UART communication with corresponding, multitude devices, inter alia, the ESCs (5). On the opposite site, the smart power board (3) with its modular LTC-boards (4) provides power to each sensor device. On Hansel, a MEMS-based INS (7) is mounted internally, whereas Gretel's FOG-aided INS is placed in an external hull. The aluminum carrier plate (6) is thermally coupled with all electrical components as well as with the top pressure hull aluminum cover for optimized heat dissipation. Standard cooling fans (8) support an even heat distribution. The interior is designed for convenient handling of each socket and clear arrangement of wirings.

alignment and positioning needs to be well known to reduce localization errors as in dead reckoning methods. Hence, the determined sensor positions are set in the design phase and are used as offset position values.

2) Communication Devices: A unique feature of the MAUS project is the variety of innovative communication solutions. For long-range communication, an acoustic modem is developed. This system is realized as a software-defined radio to adapt the transmission mode to the environmental situation. The provide rudimentary acoustic communication between vehicles and are used as a backup solution. For short to medium range communication, a magnetic modem and an optical modem were developed. For further details see Section III.

3) Surveillance and Inspection Payload: As explained above, Hansel and Gretel fulfill different purposes. Consequently, both AUVs are equipped with different sensors corresponding to their tasks. To realize the task of surveillance, Gretel's main sensor is a side-scan sonar with a maximal swath of 200 m. Each transducer is placed on both sides of the AUV (see Fig. 2) and adjusted for the maximum range. For situational awareness, Gretel uses a forward looking sonar with a maximum range of 120 m and 130° field of view. For inspection of, Hansel's payload consists of a high resolution forward looking sonar with maximum range of 10 m at 60 ° field of view. It is used for collision avoidance as well as maneuvering toward transmitted. To collect optical and spatial information of, Hansel uses a

tilt adjustable stereo camera module and a downward-facing high resolution 4 K camera. Both of the modules are in-house developments to fit the requirements for inspection like online image processing and exposure and frame rate adjustments. The stereo camera contains two industrial 1.5-MPix cameras with 4 cm baseline, pointing in the same direction. A small 1.5-GHz single-board computer triggers the cameras and calculates the disparity information by the captured images. The 4 K camera has a 12 MPix 1.1-inch sensor and a lens with 8 mm fixed focal length and variable aperture of 1.8 to 22. The lens is set to focus on objects in range 0.3–5 m. An extension board receives trigger commands from a microprocessor and forward them to the camera trigger and activates the flash light. Each camera system including extension boards and microprocessors is housed in a separate pressure hull to maintain modularity and reduce heat accumulation.

D. Software Framework

1) Overview: The execution and development of the AUV software takes place on Linux distributions, mostly Arch Linux. GitLab serves as primary platform for version control, communication, and documentation. X2Go is utilized as remote desktop software, and containerization of the software is accomplished with Podman. UpXtreme boards and Raspberry Pis are used to execute the software on the AUVs, both being single-board computers. The former boards feature more advanced CPU and graphics processing unit (GPU) capabilities, additional I/O options, as well as expandable memory and storage. One option for the AUV software was the use of the ROS. During the development of the initial software architecture at the digital signal processing group of the University of Applied Sciences in Kiel, between 2013 and 2016, ROS was not established well enough and posed various challenges. Among the challenges in those years were insufficient documentation and examples, as well as limited support for the underwater domain, since ROS 1 was mainly focused on land-based vehicles and drones. Therefore, the AUV software was developed without utilizing ROS. However, it should be noted that ROS 2, which had its first distribution release in 2017, is a viable choice for the underwater domain. The software is modular, written in C++ and compiled using Clang. The Qt software framework and its associated ecosystem are employed. Qt Pro files are utilized for software reconfiguration across different AUVs with varying hardware setups. Qt signals and slots are used to implement the main software communication system, while Qt Creator serves as IDE. In addition, ZeroMQ is partly utilized with the intention of eventually replacing Qt signals and slots. OpenCV provides a foundation for many algorithms implemented within the software. The core modules of the AUV software include: mission execution, swarm navigation and autonomy (explained in Section IV), communication (presented in Section III), object/anomaly detection, seafloor mapping (exemplified in Section V), power management (described in Section II-C), propulsion, and finally the implementation of all sensor interfaces. Fig. 5 gives an overview of the hardware and software components implemented in the AUVs.

2) Modular Design: Modular hardware and software architectures are established in AUV design and development, as evaluated and exemplified in [43] and [44]. A modular design is supposed to maintain similarity between hardware and software modules, preferably in a one-to-one relationship. This approach allows more isolated, independent development and testing of modules, while ensuring loose coupling. Integration of new modules into the software framework is straightforward. This primarily consists of including input and output of modules in the main communication system. Finally, this modular approach defines the overall capabilities of an AUV by the aggregate of all individual modules capabilities.

3) Programming Languages: The AUV software is written in established and popular C++, giving access to a vast software ecosystem. For example, it contains numerous compilers, which can perform differently, as has been shown in [45]. In general, the study of software ecosystems is a continuously evolving area of research, as has been shown by multiple literature studies [46], [47]. Finally, C++ is widely recognized as very efficient, but newer programming languages, such as TinyGo or Rust, are not lacking in terms of performance, as has been recently shown on ESP32 microcontrollers [48]. However, C++ is prone to memory safety problems, as described in [49]. Utilizing multiple programming languages in the future could enhance the flexibility of the AUV software, but creates the need for a communication system with support for all programming languages.

4) Software Frameworks: Different software frameworks are employed within the AUV software. The primary tool utilized in the development of the GUI is Qt. Furthermore, Qt modules and add-ons are used to allow for additional functionality, such as communication over networks and serial connections. OpenCV is a library mainly used for computer vision. Among the utilized features are object detection, stereopsis, motion tracking and neural networks. ZeroMQ is a messaging library, supporting numerous programming languages, transports, and patterns. To summarize, ZeroMQ allows for a more flexible approach when it comes to the modularity of the software, for instance Qt signals and slots may be used from within a single process only, ZeroMQ does not have such limitation.

5) Containerization: Containerization is the process of packaging software and all of its dependencies into a single file, called a container. Such containers are shared across the AUVs and the systems on which development takes place. This approach prevents problems that could arise from different compiler and/or library versions. The containers of the AUV software contain Arch Linux as OS, drivers, compilers, dependencies, X2Go server, XFCE desktop environment, and various IDE. Containers are supported on both x86_64 and ARM64 architectures, thereby including deployment on Raspberry Pis. Podman, a drop-in replacement for Docker, was preferred due to its native support for system development and is therefore used.

6) Software Tests: The large code base combined with complex interactions between software and hardware make it challenging to perform separate testing of the AUV software without utilizing external hardware. Tests are divided into two categories, one for tests that do not require external hardware and another for tests that do. The Google Test library is used for unit testing

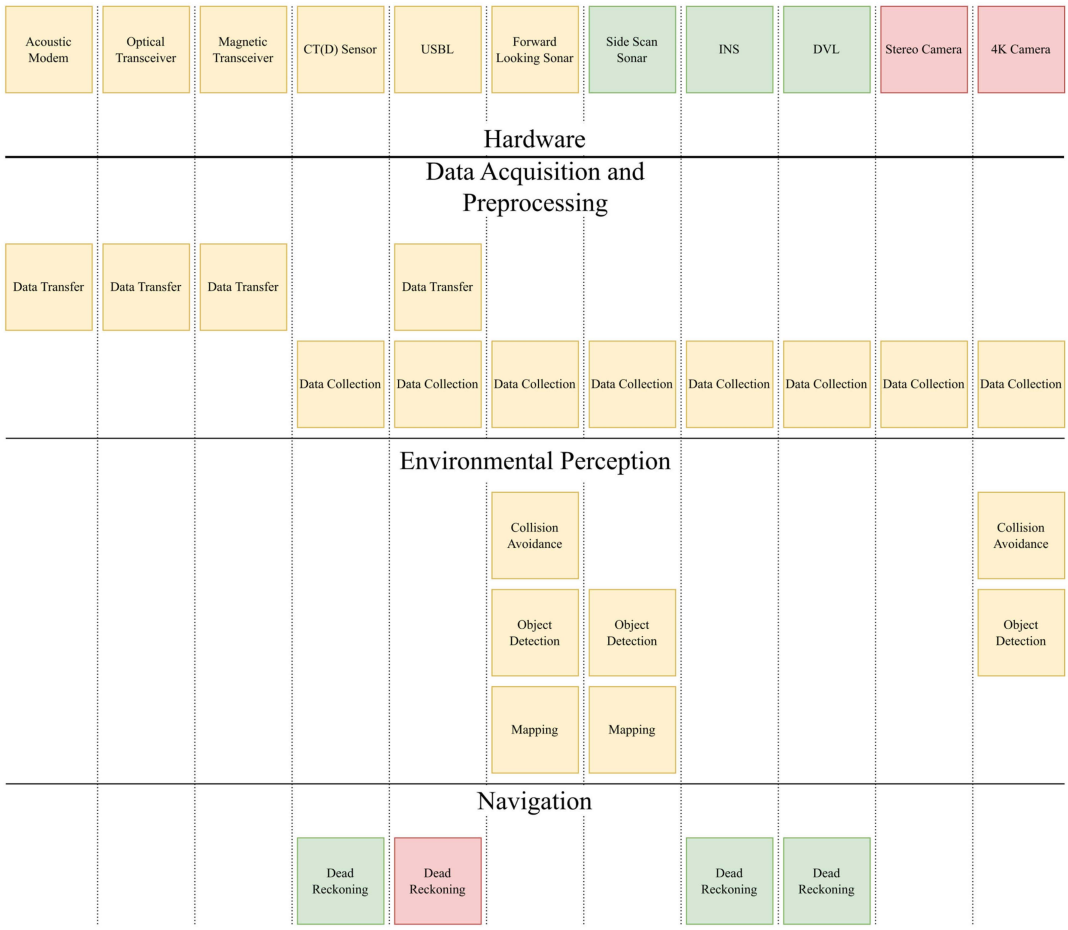

Fig. 5. Hardware components of the AUVs are horizontally aligned at the top. Hardware components implemented in both vehicles is marked in yellow, while green and red indicate hardware components unique to Gretel and Hansel, respectively. Vertically aligned are the corresponding tasks implemented in software.

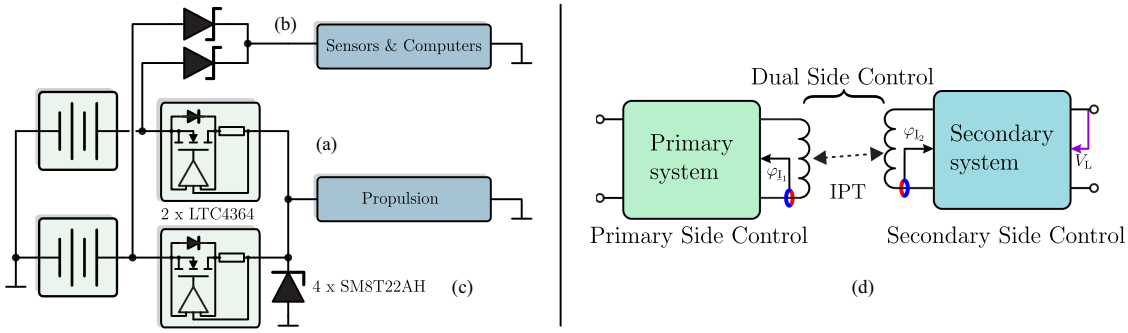

Fig. 6. Power system aspects. DC power delivery is split and managed by (a) diode emulators for the propulsion system, additional diodes (b) for low power consumers and high power suppressor diodes (c). IPT work inspired by MAUS investigates the structure of (d). The system achieves highly load independent efficiency and precision output regulation with local measurements of current phase and output voltage [51].

and mocking. Integration of the Podman container of the AUV software into GitLab CI allows tests of the first category to be executed automatically. An evaluation of challenges and suboptimal approaches related to CI has been conducted in [50].

E. Battery System and Underwater Charging

To optimize usage of internal space, the MAUS AUVs are powered by two separate, equal batteries as visualized in Figs. 1 and 2 each using an internal, manufacturer proprietary. Since the packs automatically disconnect upon system shutdown and are designed to accept charging individually via additional connectors, this presents the challenge of parallel connection upon system startup. Originally, MAUS addressed this via LTC3463 bus protection circuits featuring ideal diode emulation using discrete MOSFETs, as visualized in Fig. 6(a). The diode emulation prevents current backflow and hence equalizing currents between the packs. The chip provides auxiliary functionalities, such as an electronic fuse, for overcurrent protection.

In practice, this earlier solution causes an overvoltage issue. If the thrusters are controlled in a fashion reducing their speed at maximum rate, the rotor mechanical energy is regenerated in less than 80 ms and vastly exceeds the power consumption of the system. The excess current could not return to the batteries due to the diode emulation. The system designed for a peak bus voltage of about 25 V at full charge would experience overvoltages in excess of 30 V during regeneration, causing disruption to system operation and actual hardware damage to subsystems. This shortcoming has been solved by multiple safeguards. A digital low-pass filter in the control system is used to prevent sudden changes of the thruster speed reference values, preventing unnecessarily rapid speed changes. To prevent system damage in any case, the hardware is additionally modified as per Fig. 6. Instead of drawing power from the main propulsion bus (a), the control computers and other low power, sensitive components are isolated behind a second pair of Schottky diodes (b) in a separate quasi-isolated bus. Third, high power TVS diodes (c) such as type SM8T22AH by Eaton are connected in parallel to the propulsion system to dissipate the regenerated energy. The manufacturer leaves a significant safety margin in the breakdown voltage, therefore the 22 V type is chosen to stay below 28 V peak voltage, respecting the rating of other components. Since regeneration events are rare and constitute negligible time average energy loss, this dissipative solution is actually energy efficient, lightweight and low noise compared to a unified bus controlled by a bidirectional power converter system.

In recent years, a number of IPT systems for AUVs have been presented. The physical layout of the transfer coils in particular has been subject of thorough investigation to adapt them to the unique shapes and requirements of different AUVs. The saltwater efficiency, even though slightly reduced when compared to operation in air, is generally adequate for systems using suitable magnetic materials and frequencies below 100 kHz [52], [53]. Battery charging and general dc-bus voltages, as seen with the overvoltage problem described previously, should be tightly regulated for system safety. Since IPT has the energy transmitter and rectifier operating as separate units, control becomes an issue. Achieving high efficiency in a wide load/battery range and reliable target bus regulation requires active, local control of both system sides, i.e., DSC. This requires coordination of the system sides, on land frequently done with common radio communication standards. The saltwater environment exacerbates the communication issues and inspired a study, in which control schemes for IPT are reviewed with a focus on "communicationless" DSC schemes. These schemes provide simple, low complexity DSC in any environment and without explicit communication or complex observers/measurements. Following the review, a previously little known, remarkably simple phase cooperative DSC scheme summarized in Fig. 6(d) is investigated in depth [51]. Since phase is measured, the scheme uses a PLL for efficient synchronous low voltage rectification by default. An IPT system for MAUS based on this work is currently under construction.

III. Modem Design and Communication Strategies

In the MAUS project, data communication is based on three custom-made modems, providing an adaptation to different environments and supporting the well-known tradeoff between data rate and range. An acoustic modem is designed for long-range communication, and an inductive modem as well as an optical modem are developed for short-range communication. There are at least two reasons why short-range communication is particularly interesting in swarm systems with mobile agents: the distance between the agents is adjustable, and swarm systems preferably work in combination with docking stations for power supply and data transmission/storage. The acoustic modem serves as an umbrella cell, i.e., a robust backup link is available when short-range communication fails. This section concludes with a hybrid system concept that takes advantage of the three communication media, illustrating the range-versus-rate tradeoff in different water types.

A. Acoustic Modem

Acoustic localization and data transmission is the only option for long-range underwater wireless positioning and communication. However, due to the nonconstant speed of sound and various noise sources in water, the requirements for acoustic signal transmission are very high. Among other things, the acoustic signals are reflected, attenuated and scattered [54]. Multipath propagation affects both the localization of an object (e.g., an AUV) as well as the communication between two or more nodes (e.g., between AUVs). Commercial UAWC modems have been available off the shelf for many years. Table I lists some options. When comparing the selected acoustic modems, large specific differences between the manufacturers become apparent. Very high data rates and very high ranges are usually advertised at the same time, without pointing out the degradation of signal quality with range and channel conditions, such as shallow or deep water. Manufacturers usually do not specify the measurement parameters, so no information is given about interference and circumstances under which the stated values were achieved, or whether they were measured or calculated at all. Without further information, it can be assumed that the high data rates claimed are only achievable under very favorable conditions. Therefore, Table I should be taken with caution, as channel conditions significantly affect data rate, transmission range, and reliability. For example, maximum working range specification and maximum data rate specification cannot be achieved in the same setup.

It is important to note that besides the already mentioned disturbances and influences caused by the characteristics of the underwater transmission channel, in AUV swarms employing small vehicles the requirements are even tougher. On the one hand, the form factor needs to be small. On the other hand, the interference generated by other vehicles operating in the same frequency range is not negligible. For these reasons, a new acoustic micro-modem has been developed (see Fig. 7). This modem provides robustness under single-user conditions while being able to compensate for noise generated by the swarm agents, and is able to adapt to changing channel characteristics. A key feature of the developed modem is the SDR concept. Depending on the measured channel properties, the type of coding and modulation is selected software-based. Therefore, the data rate is adapted automatically to the transmission channel. The modem

TABLE I
OVERVIEW OF SOME COMMERCIALLY AVAILABLE ACOUSTIC MODEMS AS SPECIFIED BY MANUFACTURERS

Manufacturer/Model	Modulation	Data Rate	Frequency	Max. Range
DSPComm/AquaComm [55]	DSSS/OFDM	100–480 bps	16–30 kHz	3 km
DSPComm/Aquacomm Gen2 [56]	DSSS/OFDM	100–1000 bps	16–30 kHz	8 km
KONGSBERG/cNODE Modem Embed [57]	FSK	<6 kbps	21–31 kHz	10 km
Teledyne Benthos Atm9xx [58]	MFSK	2400 bps	18.5–24.5 kHz	6 km
AM-OFDM-S [58]	OFDM	1600 bps	21–27 kHz	4 km
WHOI Micro Modem [59]	FH-FSK/PSK	80–5400 bps	3–30 kHz	1.5 km

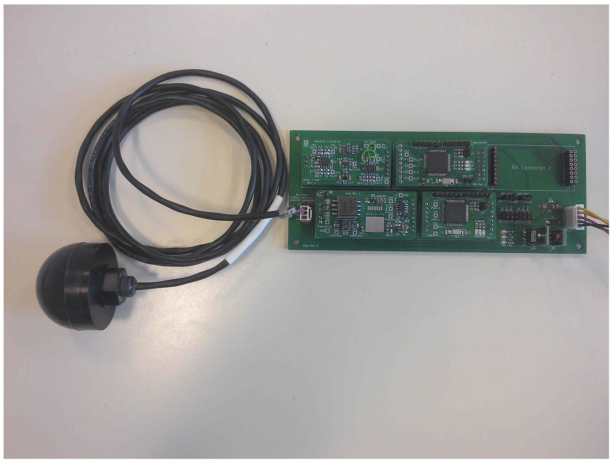

Fig. 7. Acoustic transmitter and receiver unit. The double-sided PCB houses the entire transmitting and receiving hardware, including dsPIC microcontrollers, amplifiers, and power supply peripheries. A Neptune T204 piezo transducer is connected to the PCB.

supports both single-carrier as well as multicarrier modulation methods. The latter method spreads a bit stream of fixed length over a wide frequency range. Each symbol is assigned to its own subcarrier frequency. A block can thus be transmitted at the same time, each of the bits on a different frequency. A special orthogonal modulation of the individual symbols ensures that the carriers cannot interfere with each other, i.e., intercarrier interference is minimized. Along the information bits to be transmitted, so-called pilot symbols are embedded [60]. These are known symbols, which are used on the receiving side to reconstruct the signal and restore the bit sequence. The signal processing part of the acoustic modem is implemented on 16-bit microcontrollers of the type Microchip dsPIC33ch512mp508. All calculations are performed in fixed-point arithmetic. The instruction set includes special DSP operations, and microchip provides an optimized library that performs common tasks, such as calculation and filtering. In each of the modems there are two of these microcontrollers, one for transmission and one for reception. These microcontrollers have two separate cores, one of which is permanently responsible for receiving and transmitting data to the main PC, and the other of which is permanently responsible for transmitting and receiving acoustic data through the water column. The above mentioned and implemented SDR approach can be used in particular to determine the number of bits to be transmitted per data packet, the number of bits to be transmitted per symbol, the coding and modulation mode, and the number of pilots used for synchronization and channel estimation. This makes the modem very flexible to use and easy to adapt to a wide variety of scenarios by software changes alone. On the hardware side, both an analog Class-AB amplifier and a modern and efficient Class-D amplifier are installed, and a choice can be made between their use. The transmission is done via a piezo transducer (Neptune T204) with a nominal resonant frequency of 55 kHz described in [61]. The communication with the modem is done via a serial interface, which can be accessed by any standard computer via an USB adapter.

B. Magnetic Modem

The UMWC modem utilizes magnetic fields for digital communication. Compared to the acoustic modem the communication range is small, but the data rate can be considerably higher. This technique is sensitive to the conductivity of the transmission medium but insensitive to water turbidity (including surf zones, tidal flow, and rivers), water depth, reflections by materials and surfaces, interference by sound and light, as well as Doppler spread and delay spread. In the nonradiative near field, critical issues like multipath propagation and fading are negligible. Hence, magnetic communication is even possible in shallow depths or harbor areas.

The developed UMWC modem uses an innovative system concept where the receiver coil of a conventional magneto-inductive communication system is replaced by a magnetic field detector based on four high-sensitivity wideband magnetic field sensors [33], [34]. Among other advantages, this principle enables new data modulation techniques, such as the proposed hardware/software data modulation MRFSK [62], [63], [64]. This innovative technique performs data modulation by varying the resonant frequency of the transmitter resonant circuit and has the potential to overcome several current issues encountered with other modulation schemes, such as low bandwidth, long symbol transition time, and an attenuated coil current amplitude.

1) Transmitter: The transmitter hardware shown in Fig. 8 comprises three separate main components: an amplifier board, a controllable capacitor cell circuit that also includes a high-speed zero crossing detector for either ZCS or ZVS, and a transmitter coil. The amplifier is implemented as a half-bridge inverter, converting the input voltage V_{DC} into a unipolar pulse train

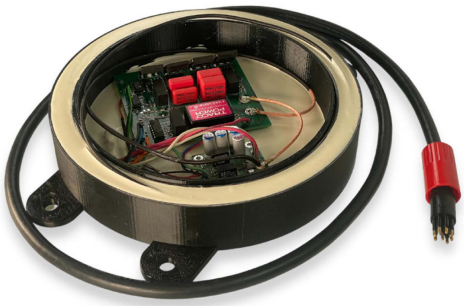

Fig. 8. UMWC transmitter consisting of an amplifier board, a controllable capacitor cell modulation circuit, and a transmitting coil. The coil is encapsulated in a pressure-neutral manner. The photo was taken for illustrative purposes before the circuit boards were encapsulated for underwater operation.

Fig. 9. UMWC receiver based on four high-sensitivity AMR broadband sensors. The signal from each sensor is amplified, spatially averaged and demodulated on board. The receiver circuitry is pressure-neutral encapsulated.

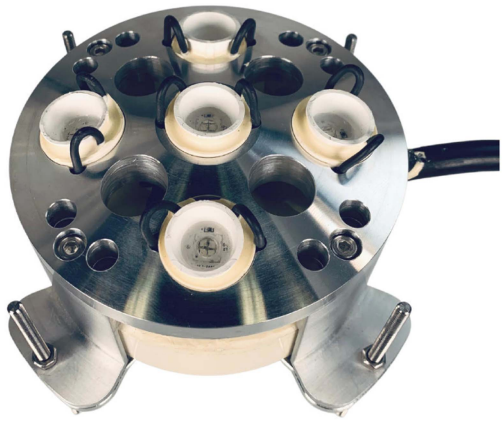

Fig. 10. Transmitter for UOWC comprising five high-power royal blue LEDs. The LED drivers are potted with thermally conductive resin and placed below the diodes which are arranged on a CNC-milled mount. This design provides optimal cooling and is space- and weight-saving.

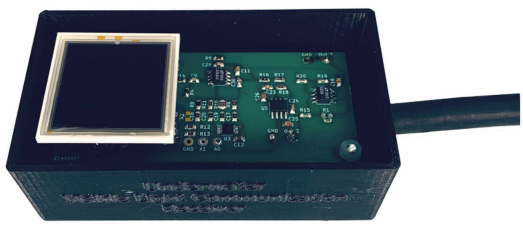

Fig. 11. Receiver for UOWC consisting of a large-area PD and a newly designed PCB for coping with several challenges such as strong signal attenuation and intense, varying sunlight. To maintain good optical properties, the unit is potted with crystal-clear polyurethane resin.

at the selected symbol frequency. The series capacitor of the resonant circuit eliminates the dc voltage component of the unipolar signal generated by the half-bridge inverter, leaving only the ac component of the square wave voltage.

The high-Q *LC* circuit (comprising the switchable capacity and transmitter coil) only permits significant current to flow at the fundamental frequency of the square wave voltage if the combination inverter switching frequency and active capacity has been chosen correctly. The ac-switches are realized by two n-channel MOSFETs each, which are arranged anti-serially. Due to the large voltages that occur in the resonant circuit, the MOSFETs have to feature a high breakdown voltage. In addition, the MOSFETs should have a low Ohmic ON-resistance to minimize the influence on the properties of the resonant circuit. These requirements are implemented via MOSFETs driven by high voltage isolating gate drivers powered from isolated dc/dc converters.

Maintaining reliable ZCS/ZVS behavior independent of precomputed timing and for parameter variation (like aging of capacitors, metal objects in the vicinity of the inductor, etc.) and potentially also for more time-efficient encoding schemes is enabled by addition of a positive-edge-triggered D-flip-flop buffer to the capacitor switch signal line. The buffer is activated by a high speed zero transition detector, based on a comparator. The comparator, outputs a high level for measured voltages greater than zero and a low level otherwise. The output signal of the comparator is additionally used for self-driving of the half-bridge inverter.

The transmitter coil is made of 23 turns of 280×0.1 mm high frequency litz wound on a printed frame with radius $r = 100$ mm. The coil is pressure-neutral encapsulated in resin for underwater applications. The inductance of the fabricated transmitter coil is 196 μH.

2) Receiver: The UMWC receiver shown in Fig. 9 is based on four Sensitec AFF755 high-sensitivity wideband low-noise magnetic field sensors. The sensibility of the AMR sensors is specified with 15 $(\text{mV/V})/(\text{kA/m})$, enabling measurements of weak magnetic flux densities in a frequency range from 0 Hz up to 1 MHz. Each of the sensing signals is amplified by an AD8428 low-noise instrumentation amplifier with a fixed gain of factor 2000. For SNR enhancement, spatial averaging is implemented on the detector board by combining the signals from all sensors. Subsequently, the signal in fed into the custom-made demodulator circuit, which supports demodulation of frequency shift keyed (FSK) and OOK signals. The signal of the demodulator output is analog-digital converted by a microcontroller and finally digitally evaluated. The outer dimensions of the receiver hardware are 98-mm length, 82-mm width, and 32-mm height.

3) Data Modulation: The data is modulated by changing the resonant frequency of the transmitter resonant circuit, which is made possible by a novel combined hardware and software

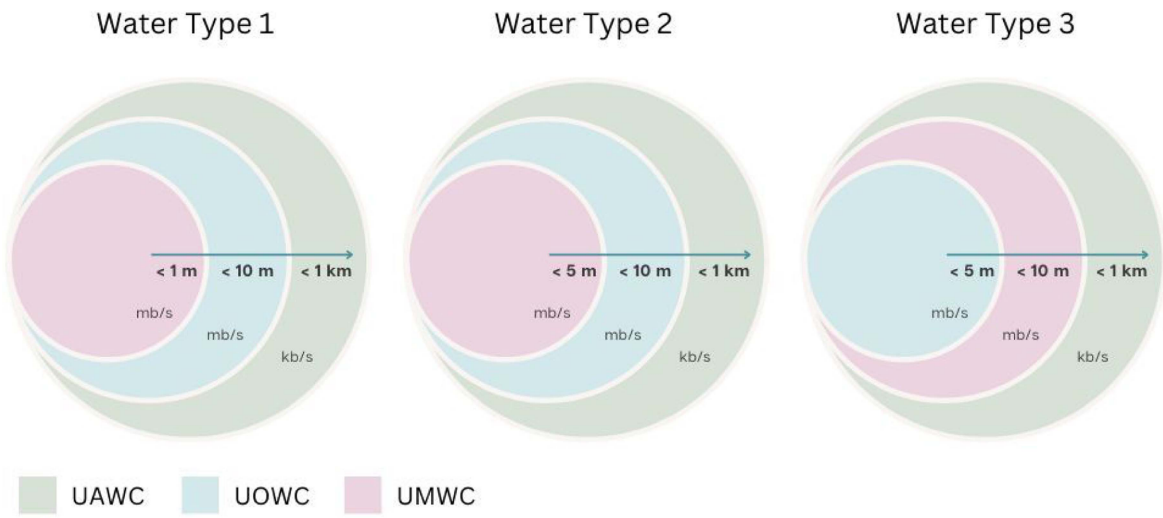

Fig. 12. Communication range for different types of water. Water type 1: Deep ocean (medium visibility and high conductivity), water type 2: Baltic Sea water (medium visibility medium conductivity), water type 3: Brackish water like in a river estuary with turbulent water (bad visibility and small conductivity).

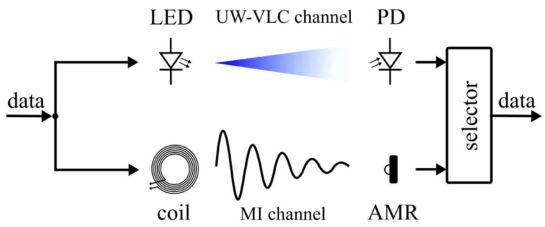

Fig. 13. Hybrid UMWC/UOWC communication system utilizing spatial diversity by transmitting the same data on both systems simultaneously.

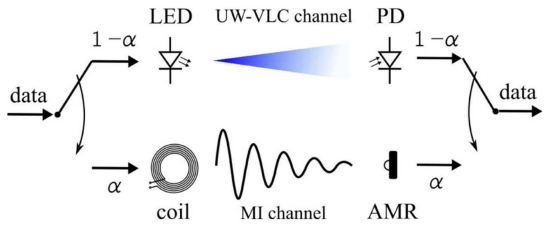

Fig. 14. Hybrid UMWC/UOWC communication system operating in hard-switching ($\alpha \in \{0, 1\}$) or soft-switching ($0 < \alpha < 1$) mode.

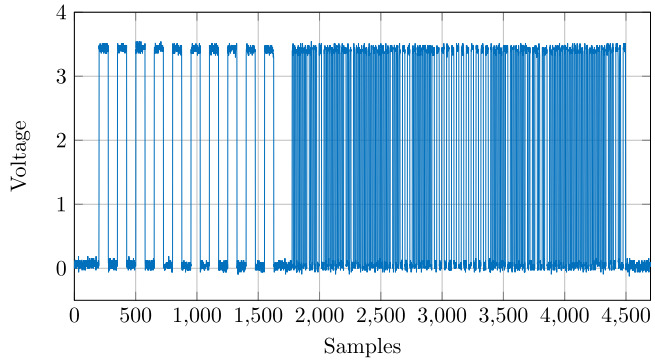

Fig. 15. Manchester-coded header received by the UOWC modem in a Baltic Sea field trial. The first ten pulses of predefined width indicate the start and are used for receiver synchronization. The header message has a length of 128 bits and is terminated by eight parity bits used for error detection.

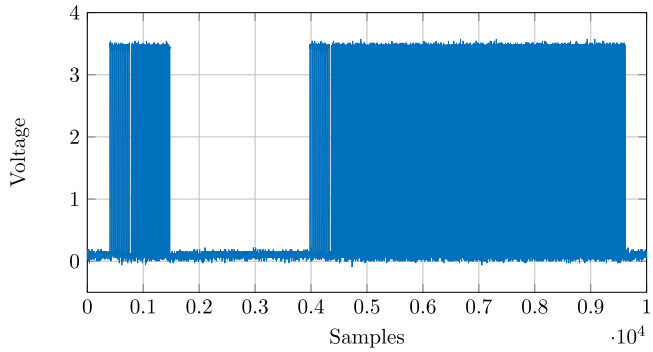

Fig. 16. Header and data packet received by the UOWC modem in a Baltic Sea field trial. As with the header, the start of the data packet is indicated by ten pulses of predetermined width. The sequence is followed by 1024 Manchester-coded data message bits plus eight parity bits for error detection.

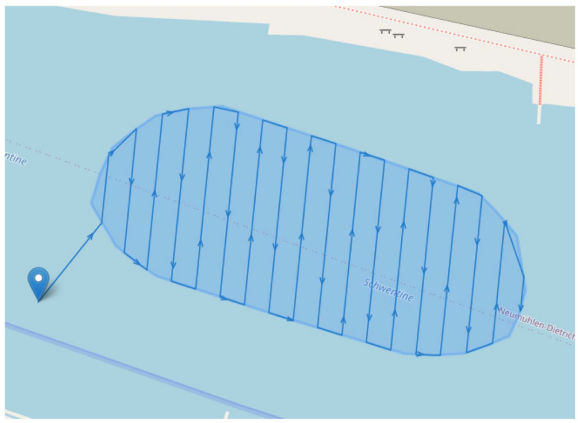

Fig. 17. Example path for CLC inside of a convex polygon. The blue marker shows the starting position of the AUV.

design approach. For the UMWC modem, a robust and easy-to-operate implementation of MRFSK is used. The hardware design provides accurate switching between two configurable resonant

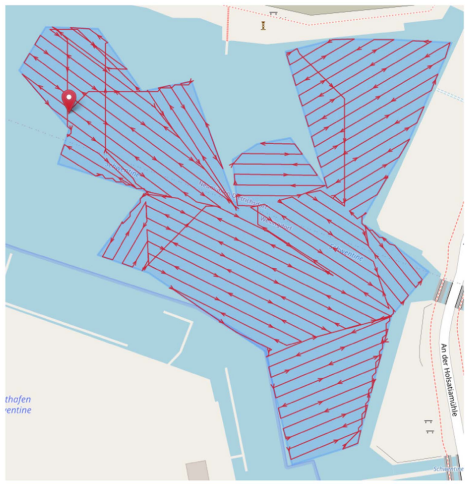

Fig. 18. For the list of convex partial polygons consisting of the ears of the original polygon, a round trip is planned via 2-opt. CLC path planning is applied to each of the subproblems.

frequencies and features an easy and a robust operation. Thanks to accurate ZVS, most of the energy of the resonant circuit can be conserved in the magnetic field of the coil during symbol changes.

C. Optical Modem

Besides the magnetic modem, an optical modem is developed for UOWC between the AUVs. It uses light in the visible range generated by [65]. In principle, are well suited for optical wireless communication due to their ability to sustain fast ON/OFF-switching [39]. This results in a high bandwidth of several MHz. Moreover, nowadays, due to the popularity in the lighting market, many different sizes, power outputs and colors, i.e., wavelengths, are available. In underwater communications, however, the selection is reduced because several limitations have to be considered.

First, the attenuation in water is considerably higher compared to air. The reason is that light is absorbed and scattered by particles in the water and by water itself [39]. Second, the signal attenuation increases, the more particles are dissolved in the water, i.e., the more turbid the water is [66]. Third, the attenuation is wavelength-dependent. As can be seen from measurements conducted in [67], the wavelength with lowest attenuation in oceanic water is between 450 nm (royal blue) and 490 nm (cyan). In coastal waters, the minimum is shifted towards yellow (575 nm) and orange (595 nm).

In conclusion, the attenuation and thus the communication range strongly depends on the quality of the water. Therefore, only high-power LEDs should be considered whose color is optimized to the expected water quality. In contrast to UMWC, however, the signal attenuation does not depend on the salinity of the water.

Therefore, a hybrid communication concept is of interest, where the UOWC approach is employed in clear, salty water conditions and is supported by the UMWC in turbid, less salty conditions [39], [68].

1) Transmitter: The developed optical transmitter depicted in Fig. 10 is equipped with five royal blue (450 nm) LED Engin LZ4 due to their high optical power, the good wall plug efficiency of 52 %, and the availability. Each LED is driven by the IXD 614, an ultrafast MOSFET driver, which offers very short rise and fall times of less than 40 ns, a wide operating voltage range and up to 14 A of drive current. The operating point of each LED is set by a current-setting power resistor. Equipping each LED with its own driver circuit has several advantages. First, the high drive current is split, which in turn distributes the load across multiple MOSFET drivers and reduces heat generation. Second, up to five separate data streams can be delivered to the optical transmitter. Thus, besides OOK, also higher order modulation schemes, e.g., 4-ASK, can be implemented straightforward. To provide sufficient cooling, the MOSFET driver and the current-setting power resistor are placed on an aluminum disc. The entire structure is then water-proofed by potting with thermally conductive resin. The are encapsulated separately. For the diode itself, crystal clear polyurethane resin is used. Both the potted driver circuit as well as the potted are placed on a CNC-milled mount made of seawater resistant AlMg3. The advantage is that both parts are surrounded by water which provides optimal cooling. Another general advantage of this structure is the space- and weight-saving design compared to conventional optical transmitters employing pressure housings. With this newly developed optical transmitter, OOK communication up to several Mbps is possible.

2) Receiver: The two main parts of the UOWC receiver shown in Fig. 11 are a large-area S3584-08 PD from Hamamatsu and a dedicated PCB for signal conversion, amplification, filtering and noise reduction. To make the unit waterproof while maintaining good optical properties, the receiver is potted with crystal clear polyurethane resin. The S3584-08 PD is chosen to capture as much light as possible with its outstanding photosensitive area of 7.84 cm^2. The sufficiently small junction capacitance is another advantage. With a reverse bias of $V_R = -15$ V a bandwidth in the MHz-region can be reached. The PD is mounted on a which is newly developed to overcome several major challenges that arise in an underwater optical communication scenario with mobile participants: the strong signal attenuation and the intense, slowly varying sunlight close to the water surface.

For this purpose, a design with multiple stages is chosen. The first stage consists of a, which is an OpAmp circuit that converts the current from the PD into a voltage and amplifies it. The amplification is given by the value of the resistor in the feedback-loop and has to be carefully selected already at this stage. If the resistor, i.e., the amplification is chosen too large, the high generated by the sunlight may be sufficient to saturate the OpAmp.

In the second stage, a high-pass filter is realized with a cut off frequency of 1 kHz. That way, only the high-frequency part of the received signal is passed to the next stage, while the and low-frequency part is canceled out. This stage is employed to combat the intense, slowly varying sunlight.

The remaining high-frequency signal that passes the high-pass filter, is further amplified by a noninverting amplifier stage. The distinctive feature of this stage is the possibility to change the amplification by switching between different resistors with a multiplexer. That way, the required amplification can be adapted to varying water quality conditions.

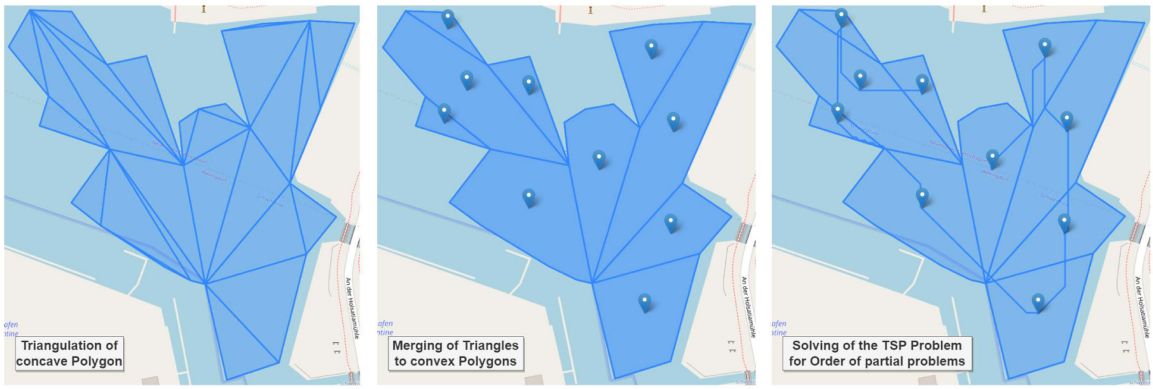

Fig. 19. Different steps of decomposition and calculation for an area of interest defined as a polygon are displayed. Since the polygon is concave, it needs to be divided into sub-problems before the coverage paths can be computed. On the left side the result of the triangulation is shown. The resulting triangles are created in several cyclical iterations around the polygon until only triangles are left. In the middle figure, these triangles are then merged if the union of two sub-polygons is still convex. This reduces the amount of problems and produces areas that are more suitable for skeleton and boustrophedon paths. In a last step a round trip for the new set of convex polygons is computed with the 2-opt algorithm.

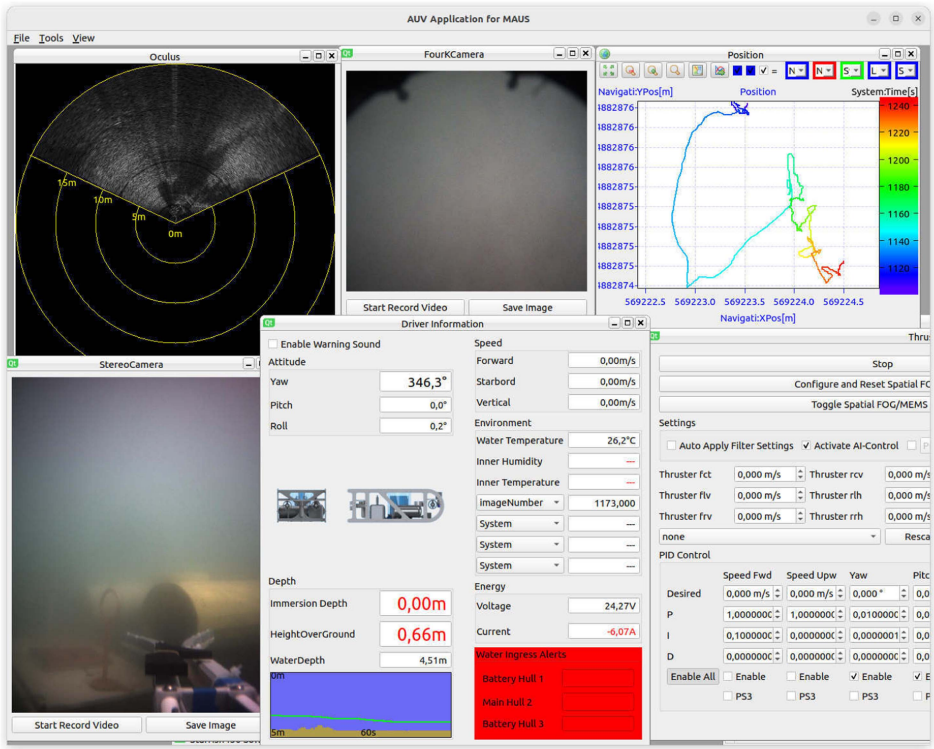

Fig. 20. GUI view showing camera images, sonar image, vehicle status, and control elements.

To improve the SNR, the third stage is followed by an active low-pass filter of second order employing the well known Sallen-Key layout. The cut off frequency is chosen as 40 MHz.

Finally, the filtered signal is passed to a noninverting Schmitt-trigger with switching hysteresis to digitalize the received signal. This has the advantage that the signal can be fed to a digital input of the subsequent microcontroller rather than into the analog input. The digital input can be read out much faster which allows for higher data rates. To avoid losing the amplitude information, the signal is also routed to an analog input before the Schmitt-trigger.

3) Data Modulation: Since generate noncoherent light and are employed to detect light intensity, the developed optical modem is restricted to IMDD. A straightforward modulation scheme of IMDD is OOK, where all five are switched ON and OFF simultaneously. The light intensities add up constructively at the receiving PD. With this technique, also other modulation schemes, such as pulse-position modulation and pulsewidth modulation can be implemented. As described above, each LED of the optical transmitter can be controlled individually. Thus, also higher order modulation schemes, such as 4- can be used.

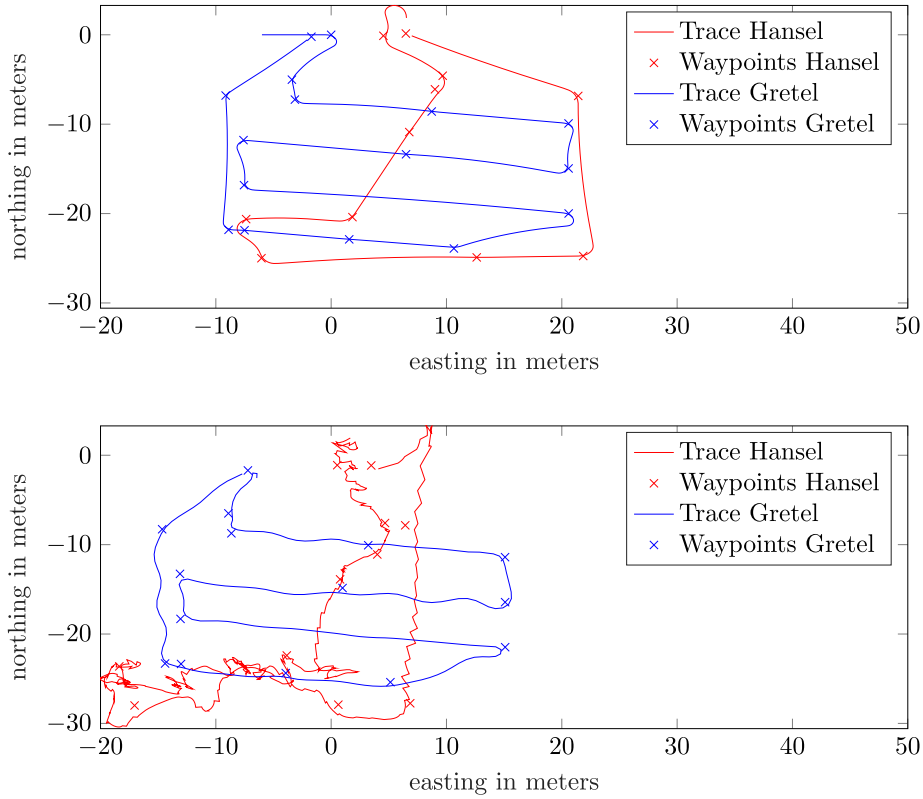

Fig. 21. Comparison of simulated (top) and real (bottom) CLC-based mission trajectory. Gretel's navigation is based on dead reckoning and Hansel navigates via USBL-aided Kalman filter. The shifted waypoints occur from error correction of the positioning results.

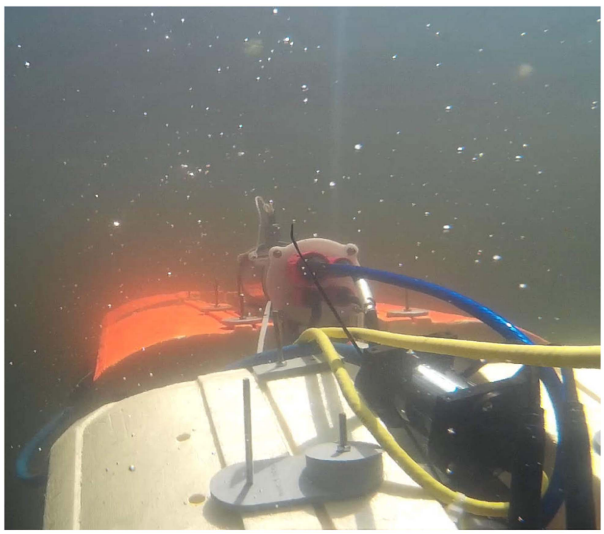

Fig. 22. Test of AUV Hansel in the Kiel Fjord. Tethering is done in the tests only, the AUV was operating fully autonomous.

D. Hybrid UAWC/UMWC/UOWC Communication Concept

As outlined above, the underwater environment is a challenging communication medium. At present, there is no universal technology that ensures a reliable and sufficiently fast underwater communication link for typical communication distances under various environmental conditions. For this reason, a combination of several techniques is required to provide a stable underwater communication link. The short range communication modem developed in the MAUS project uses both the optical and magnetic underwater channel. The combination of UMWC and UOWC is being pursued to provide a high-speed, short-range link in dynamic underwater environments. In addition, the acoustic modem serves as an umbrella cell.

On the one hand, UMWC can support UOWC in scenarios where the visibility between the transmitter and receiver is poor, i.e., in water with a high concentration of dissolved particles. On the other hand, UMWC suffers from an increasing conductivity of the transmission medium, which is associated with an increasing salt concentration of the water. In this case, UOWC can support UMWC as the attenuation is hardly dependent on the conductivity. Fig. 12 illustrates this relationship using three different example scenarios, which assume different channel conditions as follows.

1) Water Type 1: Deep ocean (medium visibility and high conductivity).
2) Water Type 2: Baltic Sea water (medium visibility medium conductivity).
3) Water Type 3: Brackish water like a river estuary with turbulent water (bad visibility and small conductivity).

Note that these example scenarios do not apply in all cases, as the channel conditions also depend on water depth, distance from the shoreline, algae growth, salinity, etc. Real-time water quality measurements are therefore advisable.

Comparing the considered scenarios previously shown, one finds that the disadvantages of one technology are outweighed by the advantages of the other: UOWC is well suited for clear waters and is little affected by salinity. UMWC, on the other hand, is not affected by water turbidity, but experiences strong attenuation in water with high salinity.

Basically, the combination of UOWC and UMWC allows two different modes of operation. The schematic in Fig. 13 outlines the first mode, where the same data are fed to both communication techniques simultaneously, thus spatial diversity is obtained.

Fig. 14 describes an adaptive approach for an efficient channel use. In this operation mode, an efficient distribution of the data stream to both communication techniques is calculated, dependent on the actual channel conditions. If the available performance of the communication techniques differs only slightly, the system operates in a soft-switching mode ($0 < \alpha < 1$). If the difference exceeds a defined threshold, only one communication method is used in a hard-switching mode $\alpha \in \{0, 1\}$. The hybrid scheme ensures an efficient use of the prevailing channel conditions. The developed communication system supports this hard switching mode, where based on the current channel conditions, the communication technique that provides the best channel capacity is selected.

To demonstrate the operation and scheduling of tasks of the hybrid communication system, let us discuss results of a mission conducted in July 2022 in the Kiel Fjord located in the southwest Baltic Sea, Germany, i.e., in Water Type 2 defined in Fig. 12. In the first step, one of the MAUS AUVs broadcasts a communication command with its acoustic modem. In addition, this command also contains the current position estimate of the vehicle. The two vehicles then begin to approach each other until high-rate communication is possible via UOWC or UMWC. In the conducted mission, the position of the first AUV is close to the water surface for the sake of supervision and inspection. The second AUV is positioned approximately 5 m below and is clearly visible. The completion of the maneuver is then communicated via the acoustic modem.

In the next step, the optical water quality is estimated. For this purpose, the optical backscattering power is measured, i.e., the amount of light emitted by an optical transmitter–receiver pair, reflected in the water column and received by the same pair. The custom-made optical transmitter–receiver pair has a distance of 10 cm and is attached to the hull of each AUV. Since a linear relationship between the backscattering power and the underwater attenuation coefficient was determined in [69], the amount of backscattered light provides good information about the water quality. In addition, the salinity is measured by the miniCT.

In the hybrid communication system used, the backscattered power is evaluated by the microcontroller, which hard-switches between UOWC and UMWC based on a threshold value. Hard-switching has a decisive advantage in mobile, energy-limited systems: the other modem can be operated in stand-by mode. In the selected Baltic Sea mission, the optical channel was chosen because Water Type 2 favors in many situations the use of the UOWC technology for short-distance high-rate communication. In brackish waters, the UMWC modem would probably have been chosen instead.

Afterward, the high-rate communication is initiated by the first AUV. Each transmission is piloted by a header and followed by a number of data packets containing up to 1024 data bits each. The header which is received at the second AUV over a distance of 5 m is depicted in Fig. 15. Due to the Schmitt-trigger, the output voltage of the received signal toggles between 0 and 3.3 V, independent of the communication distance. The same applies to the magnetic modem.

The header consists of ten start bits followed by 128 header bits plus eight parity check bits, which are all Manchester-coded, yielding a total of 292 bits. The start bits are represented by pulses with a predefined width to indicate the start of the header and to synchronize the receiver. The message bits of the header contain information regarding the selected communication technology, the modulation scheme, the chip duration, the number of data packets following the header, the AUV depth, the water salinity and the measured backscattering power.

Each data packet consists of ten start bits followed by 1024 data bits plus eight parity check bits, which are all Manchester-coded, yielding a total of 2084 bits. Fig. 16 shows the header followed by a data packet with 1024 Manchester-coded bits. Optionally, multiple data packets can be sent using a single header.

Between header and data packet as well as in-between data packets, a pause is introduced. This pause is long enough for the microcontroller to sample, decode, check, and transmit the data to the main computer via a serial interface. If an error is detected by the second AUV, an error message is transmitted instead. After either all data packets have been received or a predetermined period of time has elapsed, the main computer generates a handshake message containing either a correct reception report or the numbers of the missing or faulty data packets. This handshake message is then transmitted to the first AUV.

IV. Swarm Navigation and Autonomy

Collaborative task solving by a team of agents provides numerous advantages, including time savings, robustness, and mutually improved localization via agent communication. The risk of supplementary work must be minimized in order to reap the benefits of collaborative behavior. The goal should be to use multiple agents to reduce the total duration of the mission, making it more energy-efficient, while also balancing the load of the individual agents to use all robots efficiently.

As a heterogeneous team, Hansel and Gretel can perform various tasks jointly and autonomously. The goal is to find the best task distribution for the agents. In most cases, the workspace is known ahead of time, and only area-wide measurements are required. Choosing the best path for a collaborative team of robots in terms of energy efficiency, on the other hand, is a computationally difficult problem. The following subsections will introduce the AI-guided navigation including the automated mission path planning as well as the autonomous execution of tasks.

```
<mission name=search_fjord auv=gretel>
    <task id=1 optionalid=3 timeout=2000 name=approach_start_point>
        <goto easting=50 northing=100 id=1 nextid=2 optionalid=5 timeout=1200 />
        <goto easting=100 northing=100 id=2 nextid=3 optionalid=5 timeout=1200 />
    </task>
    <task id=2 optionalid=3 timeout=36000 name=search>
        <find easting=200 northing=200 id=3 nextid=5 optionalid=4 timeout=3600 />
        <find easting=300 northing=300 id=4 nextid=5 optionalid=3 timeout=3600 />
    </task>
    <task id=3 optionalid=0 timeout=5000 name=return_to_home>
        <goto easting=100 northing=100 id=5 nextid=0 optionalid=0 timeout=2000 />
    </task>
```

A. *Structure and Execution of Commands*

To follow the subsequent approach, it is necessary to understand how the AUVs realize a mission. A set of commands, such as `goto`, `pause`, `acknowledge`, `waitforacknowledge`, and `find`, are the base for all *tasks*. A detailed explanation of all commands can be found in [70]. A *task* is defined by a list of commands that subjectively form a higher level action. Each command is described by its target parameters, a unique identifier, the identifier of the subsequent command, an optional-identifier that is per default 0, and an optional timeout. The term *optional* in optional-identifier is meant to be the alternative subsequent command if the intended subsequent command cannot be reached due to failure of the current command. Each mission starts by the execution of command with identifier 1 and is terminated if the current identifier is 0. Supposing that a command succeeds, the command that is set as subsequent identifier is next active. If a command fails or a timeout occurs, the command with the optional-identifier is executed next instead. This enables situation-based decisions, which is elementary for search missions, for example. This list is extendable during mission time by adding instructions with unique identifiers or skipping commands by changing the linked subsequent command. Each task has also its own unique identifier, a name, an optional timeout and an optional identifier per default set to 0. The name is mainly used for post mission analysis, whereas the other parameters serve the following purpose. In case a command inside of a task is active, the task timer continues ticking. If a tasks timer runs out, the first command of the task with the optional identifier is executed. This helps to prevent infinite loops and limits the overall possible mission time. All tasks for one team member are grouped by a mission header that defines member specific mission parameters. To realize a unique mission assignment, all team-specific mission headers are listed in a single mission file, with mission-specific confirmation identifiers in a meaningful context. A small example demonstrates the presented functionality:

The mission consists of three tasks, namely, `approach_start_point`, `search`, and `return_to_home`. If the first task timer runs out or a contained command fails, the `return_to_home` task is started. Otherwise, the second task starts, where an OOI has to be found. This operation continues, as long as the OOI is not found and the task timer does not run out. This is achieved by the mutual invocation of the `find` commands.

B. *Creeping Line Search Path Planning*

There are several ways to form teams or swarms that are modeled after SAR maneuvers described in the annual IAMSAR manual [71]. The CLC is a very efficient variation, in which a swarm member (Gretel) traverses back-and-forth search sections parallel to each other based on the scan width of its sensors. The goal is to cover the entire survey area without using redundant paths. These paths, as seen in Fig. 17, are simple to compute for work spaces defined by convex polygons. However, because there are frequently areas that cannot be navigated, such as jetties in harbors or fixed fishing nets, the working space often must be specified by concave polygons.

C. *Path Planning for Complex-Shaped Search Areas*

Because of the indentations in concave polygons, planning the search sections is extremely complicated if redundant paths are to be avoided. The high space and time complexity required to solve the coverage problem is a major issue with current methods. A grid map is frequently created for the data representation of the workspace. As the resolution or size of the workspace increases, so do the memory requirements. The coverage problem is usually too complex to solve in real time. As a result, an approach is taken to decompose the workspace efficiently using algorithmic geometry methods. The workspace is divided into triangles by using a modified ear-clipping algorithm based on the fast industrial-strength triangulation (FIST) method, allowing for easier handling of the resulting convex polygons [72].

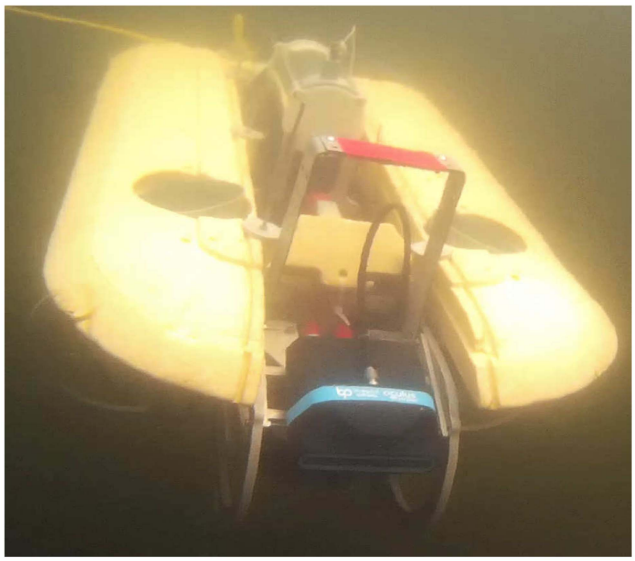

Fig. 23. Test of AUV Gretel in the Kiel Fjord. With regard to tethering, the same applies as for Hansel.

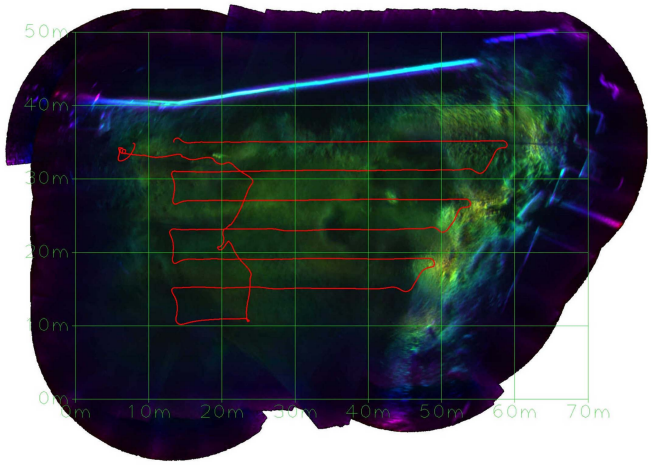

Fig. 24. Sonar map as a result from test in open water. The color corresponds the pixels closest range to the vehicle and can be interpreted as bottom height. The red line in the map indicates the trajectory of the AUV.

If the union is also convex, adjacent polygons are connected for even more simplification. The new workspace division is not necessarily optimal, but it can be computed quickly. The centers of the newly created convex polygons for neighbors are then connected to form a topological map. The 2-opt algorithm can then be used to determine the optimal order of coverage [73], see Fig. 19 for the subsequent steps of the decomposition. For each section, only the parallel search sections are planned. A complete CLC path for a concave work environment is depicted in Fig. 18 [74].

To assist end users such as marine researchers in planning AUV missions, a GUI was developed within the MAUS project, see Fig. 20. This GUI supports to plan missions with little effort and prior knowledge for a heterogeneous team of agents and thus to solve the targeted mission efficiently. The necessary tasks are distributed by the GUI to the agents. By setting features of each agent, the GUI provides a mission file including time estimation of each command and task. It is also capable to receive online mission data and follow the state of the current mission. This provides a reasonable overview, especially in dynamic mission sections.

D. CLC-Based Workflow

Gretel sends the positions of potential objects of interest to Hansel during the scan so that they can be thoroughly examined. Hansel is well-equipped for the inspection tasks, but it can only be located in relation to Gretel using USBL. Since Hansel is not supposed to follow Gretel, it requires knowledge of possible positions that minimize the average distance between the AUVs. As a result, Gretel sends Hansel acknowledgment messages with unique identifiers, indicating the current search leg of the mission. Hansel will remain at its synchronization point as long as it does not receive an acknowledgment message or a time-out occurs. Gretel sends the acknowledgment message when it reaches its synchronization point. If necessary, the AUVs can be positioned above each other via the synchronization points, enabling the exchange of a vast amount of information via magnetic or optical communication. Furthermore, mutual synchronization by sending and expecting an acknowledgment are set between tasks. Fig. 21 depicts an example mission with a specific CLC pattern and paths for each agent type. A further issue of the USBL-modem internal localization is that it cannot provide continuous position information for the requesting AUV. Therefore, Hansel receives a position update only each 5 to 10 s. In between those position updates, Hansel's Kalman filter estimates its position solely on MEMS data. Under the influence of currents and sensor inaccuracies this may result in a sawtooth-shaped trajectory, as shown in Fig. 21. As a result and due to other measurement inaccuracies, Hansel may miss the true position of the OOI. One option is to transmit object-specific features of the OOI via one of the developed modems, allowing Hansel to detect and localize the position of the OOI in order to correct its planned path. Because the amount of data per message is severely limited if the acoustic modem is taken, in [70] a method was proposed to compress the object information into a short vector. Although the basic swarm navigation concept is conceptualized for two types of vehicles, a third surface-based type, namely, an USV, has been developed in the framework of the MAUS project to support the underwater vehicles with telemetry data and forwards status messages to the mission control GUI and hence to the operator. Buoys and submerged anchors are alternatives.

V. Field Trials and Experimental Results

Testing within the MAUS project was done continuously. Since different partners were involved, individual modules were first tested separately in the corresponding institute laboratories. The integration of all modules in the AUVs and joint tests were carried out in the AUV laboratory at Kiel University of Applied Sciences. There, simple tests, such as leak testing, control, and regulation of the thrusters, navigation system of the vehicles, transmitting and receiving units, etc., were carried out in a tank. Additional tests were carried out in an outdoor swimming pool

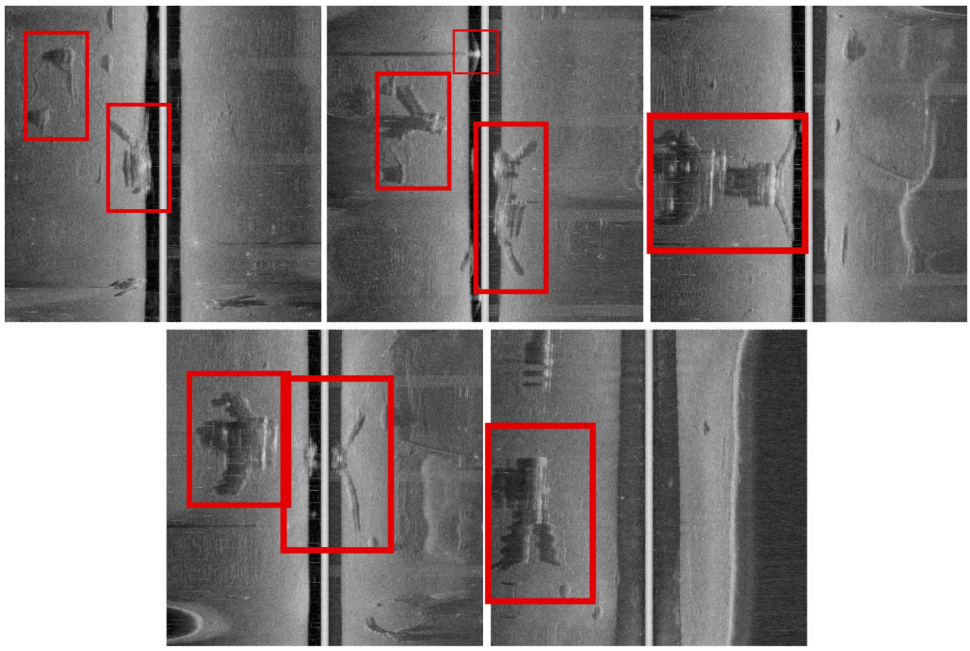

Fig. 25. Side-scan sonar waterfall images of different underwater objects, indicated by red bounding boxes.

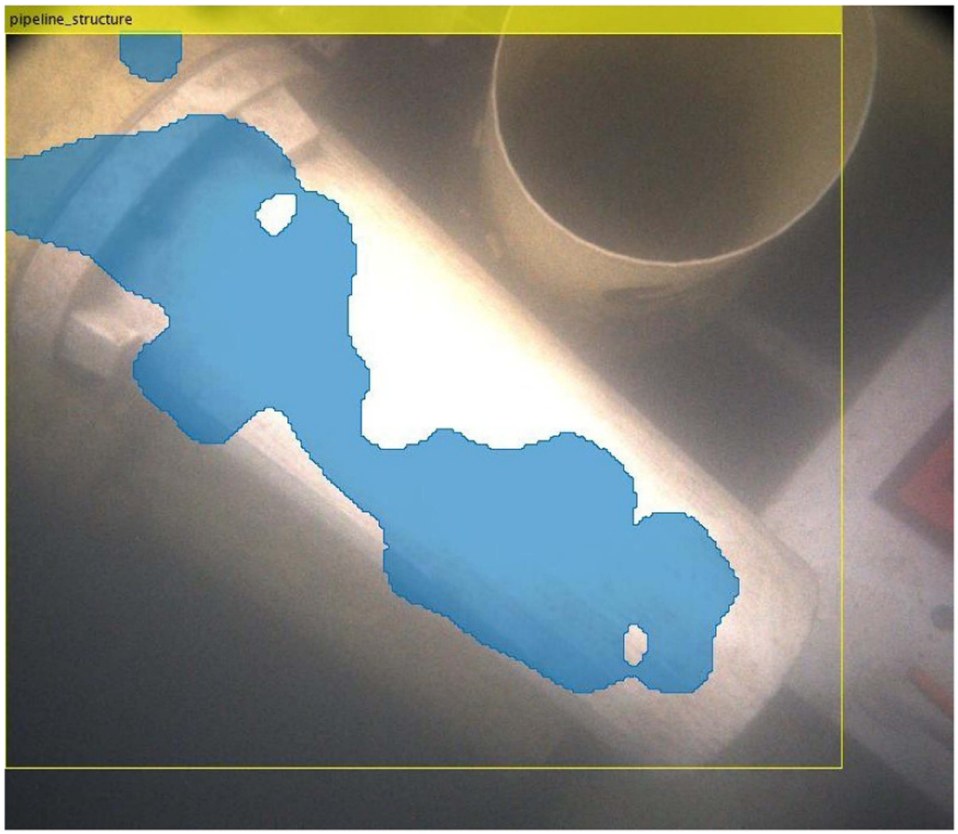

Fig. 26. Detection of underwater structures in the 4 K camera.

to check the sensor technology including sonar and camera data as well as the acoustic, magnetic and optical data transmission. After completion of these tests, the AUVs were tested in open waters in the Kiel Fjord and in a harbor basis at La Spezia, Italy. The entire MAUS system was validated under different conditions and scenarios. Figs. 22 and 23 show an autonomous diving process of Hansel and Gretel in the Kiel Fjord taking pictures of each other. The resulting sonar map of the open water test is plotted in Fig. 24. This mosaic is utilized in the subsequent examination of the search area and exhibits a high

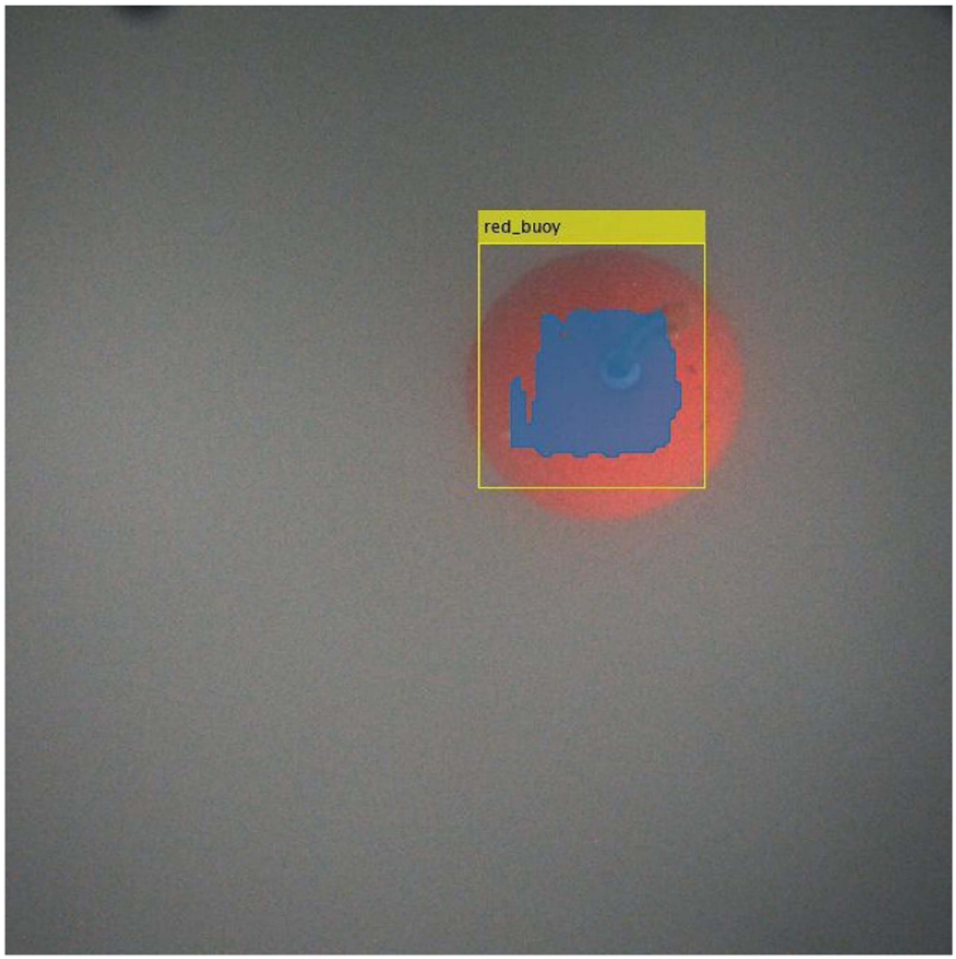

Fig. 27. Detection of a red buoy in the 4 K camera.

degree of sensitivity in identifying anomalies. The basic concept of swarm navigation is simulated and tested multiple times in a scaled-down version as depicted in Fig. 21 for the Kiel Fjord. In this test scenario, the AUVs perform their mission as described in [70]. Gretel moves in a lawn-moving pattern and searches for anomalies. If an OOI is found, a message containing position information is sent to Hansel. Hansel's mission control module inserts this new target as a new subsequent job and inspects it. In this specific test the occurrence of the anomaly in Gretel's sensors is triggered artificially to test and compare the cooperative behavior in a determined manner. In the displayed scenario, the OOI occurs at the bottom left side of the test area. As planned, Hansel follows Gretel along the northing axes and waits at the previously described synchronization points for Gretel's transit. In Gretel's last search leg, an (artificial) OOI is communicated to Hansel via USBL and animates Hansel to inspect the new target. After Hansel reached the desired target waypoint, it returns to continue its previous mission schedule. In the tests, Hansel and Gretel performed as expected, although Hansel's navigation struggled through water currents and disturbed position updates due to the shallow water. Due to the shallow depth of the water of about 2–5 m, maintaining a stable acoustic communication and USBL link becomes problematic and causes navigation challenges. Despite these difficulties, both AUVs are capable of accomplishing the mission.

The assessment of sensor capabilities and object detection is conducted in La Spezia, Italy, where a harbor basin was specifically arranged with simulated underwater structures and debris, including buoys, pipes, and consoles. The maximum water depth of the basin is 9 m, and the AUVs are customized for optimal object capture within this range. The use of side-scan imagery, which is a crucial function of Gretel, necessitates a consistent velocity along a straight path. In Fig. 25, various side-scan waterfall images featuring highlighted anomalies are presented. The images exhibit only few distorted objects, suggesting a stable motion behavior during data acquisition. Next, the configurations of the cameras are evaluated, and anomaly detection are tested. The structure is captured using both the stereo camera system (depicted in the GUI in Fig. 20) and the 4 K camera system presented in Fig. 26. The object detectors, which were primarily applied to the 4 K camera images, were assessed using various deep learning approaches such as MASK-RCNN [75]. These approaches were trained on different underwater structures, mainly of human origin, such as pipes and buoys (see Figs. 26 and 27). Currently, the YOLOv5 [76] is the preferred approach for analyzing data obtained from

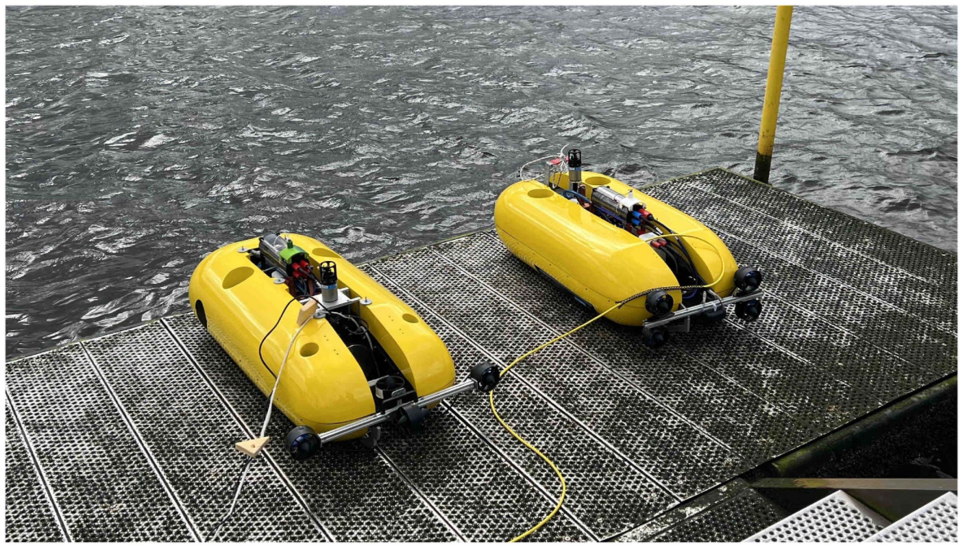

Fig. 28. Hansel (left) and Gretel (right) during tests in the Kiel Fjord.

the 4 K camera, side-scan sonar, and forward-looking sonar. However, newer versions of the approach are being investigated.

In addition to the tests for navigation, localization, communication, and autonomy in connection with the swarm principle, procedures for object detection, collision avoidance with the sonar and camera data were also developed, tested and optimized [70], [77].

VI. Conclusion

In this article, we summarize the scientific results of the collaborative EU.SH project MAUS', targeting the hardware and software design, cooperation, mission planning and hybrid communication strategy for a multiheterogeneous AUV swarm. Focus is on two AUV types equipped with different sensor technology, which complement each other with respect to their application possibilities: a hovering vehicle ("Hansel") and a going vehicle ("Gretel"), see Fig. 28. The vehicles are characterized by a high degree of modularity, a small size, comparatively low cost, and cooperation. Innovative features include a hybrid communication concept based on acoustic, magnetic, and optical communication. Communication between the swarm elements improves localization accuracy. Furthermore, novel AI-based approaches for route planning, mission description and task solving are presented, which are efficiently applicable for arbitrary deployment areas. Experimental verification has been performed in the Kiel Fjord, located in the southwest Baltic Sea, and in La Spezia, Mediterranean Sea.

This work has addressed many principles and tasks of swarm collaboration with two different, cooperating AUVs that complement each other. This has created a platform that is open for further improvements and enhancements. The extension to more than two vehicles is taken into account in the concept.

Acknowledgment

The authors would like to thanks the support of Alexander Bartsch, Andreas Kaschube, Bjoern Lehmann-Matthaei, Jan Paul, Peer Poggendorf, Uwe Ruhland, Katharine Wichelmann, Lars Wolff, and Paul Wrobel.

References

[1] G. Griffiths, *Technology and Applications of Autonomous Underwater Vehicles*. Boca Raton, FL, USA: CRC Press, 2002.
[2] S. Wadoo and P. Kachroo, *Autonomous Underwater Vehicles: Modeling, Control Design and Simulation*. Boca Raton, FL, USA: CRC Press, 2017.
[3] F. Ehlers, *Autonomous Underwater Vehicles: Design and Practice*, SciTech Publishing, 2020.
[4] J. Yan, X. Yang, H. Zhao, X. Luo, and X. Guan, *Autonomous Underwater Vehicles: Localization, Tracking, and Formation*. Berlin, Germany: Springer, 2021.
[5] H. Hamann, *Swarm Robotics: A. Formal Approach*. Berlin, Germany: Springer, 2018.
[6] M. Schranz, M. Umlauft, M. Sende, and W. Elmenreich, "Swarm robotic behaviors and current applications," *Front. Robot. AI*, vol. 7, 2020, Art. no. 36.
[7] D. Payton, M. Daily, B. Hoff, M. Howard, and C. Lee, "Pheromone robotics," *Auton. Robots*, vol. 11, pp. 319–324, 2001.
[8] C. Beni, "From swarm intelligence to swarm robotic," in *Proc. Workshop Swarm Robot.*, 2005, 3342, pp. 1–9.
[9] M. Brambilla, E. Ferrante, M. Birattari, and M. Dorigo, "Swarm robotics: A review from the swarm engineering perspective," *Swarm Intell.*, vol. 7, pp. 1–41, 2013.
[10] F. WeiXing, W. KeJun, Y. XiuFen, and G. ShuXiang, "Novel algorithms for coordination of underwater swarm robotics," in *2006 IEEE Int. Conf. Mechatron. Autom.*, 2006, pp. 654–659.
[11] M. A. Joordens and M. Jamshidi, "Underwater swarm robotics consensus control," in *2009 IEEE Int. Conf. Syst., Man, Cybern.*, 2009, pp. 3163–3168.
[12] S. Dai, Z. Wu, P. Zhang, M. Tan, and J. Yu, "Distributed formation control for a multi-robotic fish system with model-based event-triggered communication mechanism," *IEEE Trans. Ind. Electron.*, vol. 70, no. 11, pp. 11433–11442, Nov. 2023.
[13] T. Schmickl et al., "CoCoRo-The self-aware underwater swarm," in *2011 5th IEEE Conf. Self-Adaptive Self-Organizing Syst. Workshops*, 2011, pp. 120–126.

[14] C. Osterloh, T. Pionteck, and E. Maehle, "MONSUN II: A small and inexpensive AUV for underwater swarms," in *2012 7th VDE German Conf. Robot.*, 2012, pp. 1–6.

[15] A. Hackbarth, E. Kreuzer, and E. Solowjow, "HippoCampus: A micro underwater vehicle for swarm applications," in *2015 IEEE/RSJ Int. Conf. Intell. Robots Syst.*, 2015, pp. 2258–2263.

[16] M. Carreras, J. D. Hernández, E. Vidal, N. Palomeras, D. Ribas, and P. Ridao, "Sparus II AUV: A hovering vehicle for seabed inspection," *IEEE J. Ocean. Eng.*, vol. 43, no. 2, pp. 344–355, Apr. 2018.

[17] S. Iacoponi et al., "H-SURF: Heterogeneous swarm of underwater robotic fish," in *2022 IEEE/MTS OCEANS*, Hampton Roads, VA, USA, 2022, pp. 1–5.

[18] S. Zhang, R. Pöhlmann, T. Wiedemann, A. Dammann, H. Wymeersch, and P. A. Hoeher, "Self-aware swarm navigation in autonomous exploration missions," *Proc. IEEE*, vol. 108, no. 7, pp. 1168–1195, Jul. 2020.

[19] R. Alghamdi, H. Dahrouj, T. Al-Naffouri, and M.-S. Alouini, "Toward immersive underwater cloud-enabled networks: Prospects and challenges," *IEEE BITS Inf. Theory Mag.*, vol. 3, no. 2, pp. 54–66, Jun. 2023.

[20] B. T. Champion and M. A. Joordens, "Underwater swarm robotics review," in *2015 10th IEEE Syst. Syst. Eng. Conf.*, 2015, pp. 111–116.

[21] G. Liu, L. Chen, K. Liu, and Y. Luo, "A swarm of unmanned vehicles in the shallow ocean: A survey," *Neurocomputing*, vol. 531, pp. 74–86, 2023.

[22] N. Vedachalam, R. Ramesh, V. B. N. Jyothi, V. Doss Prakash, and G. Ramadass, "Autonomous underwater vehicles-challenging developments and technological maturity towards strategic swarm robotics systems," *Mar. Georesources Geotechnol.*, vol. 37, no. 5, pp. 525–538, 2019.

[23] N. Vedachalam, R. Ramesh, V. B. N. Jyothi, V. D. Prakash, G. A. Ramadass, and M. A. Atmanand, "Design considerations for strategic autonomous underwater swarm robotic systems," *Mar. Technol. Soc. J.*, vol. 54, no. 2, pp. 25–34, 2020.

[24] J. Connor, B. Champion, and M. A. Joordens, "Current algorithms, communication methods and designs for underwater swarm robotics: A review," *IEEE Sensors J.*, vol. 21, no. 1, pp. 153–169, Jan. 2021.

[25] K. S. Keerthi, B. Mahapatra, and V. G. Menon, "Into the world of underwater swarm robotics: Architecture, communication, applications and challenges," *Recent Adv. Comput. Sci. Commun.*, vol. 13, no. 2, pp. 110–119, 2020.

[26] A. Luvisutto, A. Al Shehhi, N. Mankovskii, F. Renda, C. Stefanini, and G. De Masi, "Robotic swarm for marine and submarine missions: Challenges and perspectives," in *Proc. IEEE/OES Auton. Underwater Veh. Symp.*, 2022, pp. 1–8.

[27] Z. Sun and I. F. Akyildiz, "Magnetic induction communications for wireless underground sensor networks," *IEEE Trans. Antennas Propag.*, vol. 58, no. 7, pp. 2426–2435, Jul. 2010.

[28] M. C. Domingo, "Magnetic induction for underwater wireless communication networks," *IEEE Trans. Antennas Propag.*, vol. 60, no. 6, pp. 2929–2939, Jun. 2012.

[29] Z. Sun, I. F. Akyildiz, S. Kisseleff, and W. Gerstacker, "Increasing the capacity of magnetic induction communications in RF-challenged environments," *IEEE Trans. Commun.*, vol. 61, no. 9, pp. 3943–3952, Sep. 2013.

[30] I. F. Akyildiz, P. Wang, and Z. Sun, "Realizing underwater communication through magnetic induction," *IEEE Commun. Mag.*, vol. 53, no. 11, pp. 42–48, Nov. 2015.

[31] B. A. Belyaev et al., "Compact non-linear power amplifier for wideband underwater and underground near-field magnetic communication systems," in *2019 IEEE Int. Siberian Conf. Control Commun.*, 2019, pp. 1–5.

[32] S. Ryu et al., "Design and analysis of a magnetic field communication system using a giant magneto-impedance sensor," *IEEE Access*, vol. 10, pp. 56961–56973, 2022.

[33] M. Hott, P. A. Hoeher, and S. F. Reinecke, "Magnetic communication using high-sensitivity magnetic field detectors," *Sensors*, vol. 19, no. 15, 2019, Art. no. 3415.

[34] M. Hott and P. A. Hoeher, "Underwater communication employing high-sensitive magnetic field detectors," *IEEE Access*, vol. 8, pp. 177385–177394, 2020.

[35] H. Kaushal and G. Kaddoum, "Underwater optical wireless communication," *IEEE Access*, vol. 4, pp. 1518–1547, 2016.

[36] Z. Zeng, S. Fu, H. Zhang, Y. Dong, and J. Cheng, "A survey of underwater optical wireless communications," *IEEE Commun. Surv. Tut.*, vol. 19, no. 1, pp. 204–238, Firstquarter 2017.

[37] N. Saeed, A. Celik, T. Y. Al-Naffouri, and M.-S. Alouini, "Underwater optical wireless communications, networking, and localization: A survey," *Ad Hoc Netw.*, vol. 94, Nov. 2019, Art. no. 101935.

[38] F. Campagnaro, A. Signori, and M. Zorzi, "Wireless remote control for underwater vehicles," *J. Mar. Sci. Eng.*, vol. 8, no. 10, 2020, Art. no. 736.

[39] P. A. Hoeher, J. Sticklus, and A. Harlakin, "Underwater optical wireless communications in swarm robotics: A tutorial," *IEEE Commun. Surv. Tut.*, vol. 23, no. 4, pp. 2630–2659, Fourthquarter 2021.

[40] J. Wang, W. Shi, L. Xu, L. Zhou, Q. Niu, and J. Liu, "Design of optical-acoustic hybrid underwater wireless sensor network," *J. Netw. Comput. Appl.*, vol. 92, pp. 59–67, 2017.

[41] G. N. Arvanitakis et al., "Gb/s underwater wireless optical communications using series-connected GaN micro-LED arrays," *IEEE Photon. J.*, vol. 12, no. 2, Apr. 2020, Art. no. 7901210.

[42] J. Sola, "Quaternion kinematics for the error-state Kalman filter," 2017, *arXiv:1711.02508*.

[43] M. Sangekar, M. Chitre, and T. B. Koay, "Hardware architecture for a modular autonomous underwater vehicle STARFISH," in *Proc. IEEE/MTS OCEANS*, Quebec City, Canada, Sep. 2008, pp. 1–8.

[44] P. A. Gutierrez-Flores and R. Bachmayer, "Concept development of a modular system for marine applications using ROS2 and micro-ROS," in *2022 IEEE/OES Auton. Underwater Veh. Symp.*, Singapore, Sep. 2022, pp. 1–6.

[45] K. Halbiniak, R. Wyrzykowski, L. Szustak, A. Kulawik, N. Meyer, and P. Gepner, "Performance exploration of various C/C compilers for AMD EPYC processors in numerical modeling of solidification," *Adv. Eng. Softw.*, vol. 166, Apr. 2022, Art. no. 103078.

[46] K. Manikas, "Revisiting software ecosystems research: A longitudinal literature study," *J. Syst. Softw.*, vol. 117, pp. 84–103, Jul. 2016.

[47] K. Manikas and K. M. Hansen, "Software ecosystems: A systematic literature review," *J. Syst. Softw.*, vol. 86, no. 5, pp. 1294–1306, May 2013.

[48] I. Plauska, A. Liutkevičius, and A. Janavičiūtė, "Performance evaluation of C/C, MicroPython, Rust and TinyGo programming languages on ESP32 microcontroller," *Electronics*, vol. 12, no. 1, Dec. 2022, Art. no. 143.

[49] Y. Jeon, "Practical type and memory safety violation detection mechanisms," Ph.D. dissertation, Dept. of Comput. Sci., Purdue Univ., West Lafayette, IN, USA, 2020.

[50] R. B. T. Silva and C. I. M. Bezerra, "Analyzing continuous integration bad practices in closed-source projects," in *2020 34th Braz. Symp. Softw. Eng.*, Oct. 2020, pp. 642–647.

[51] J. M. Placzek, H. Beiranvand, and M. Liserre, "Communicationless phase cooperative control of inductive power transfer using asymmetrical modulations," *IEEE Trans. Power Electron.*, vol. 38, no. 6, pp. 7836–7847, Jun. 2023.

[52] C. R. Teeneti, T. T. Truscott, D. N. Beal, and Z. Pantic, "Review of wireless charging systems for autonomous underwater vehicles," *IEEE J. Ocean. Eng.*, vol. 46, no. 1, pp. 68–87, Jan. 2021.

[53] C. Cai, S. Wu, Z. Zhang, L. Jiang, and S. Yang, "Development of a fit-to-surface and lightweight magnetic coupler for autonomous underwater vehicle wireless charging systems," *IEEE Trans. Power Electron.*, vol. 36, no. 9, pp. 9927–9940, Sep. 2021.

[54] M. Stojanovic and J. Preisig, "Underwater acoustic communication channels: Propagation models and statistical characterization," *IEEE Commun. Mag.*, vol. 47, no. 1, pp. 84–89, Jan. 2009.

[55] "AQUACOMM: Underwater acoustic modems." (n.d.). [Online]. Available: https://www.dspcommgen2.com/aquacomm-gen2-next-generation-acoustic-modem/

[56] "AQUACOMM GEN2: Next generation underwater wireless modem." (n.d.). [Online]. Available: https://www.dspcommgen2.com/aquacomm-gen2-next-generation-acoustic-modem/

[57] "Maritime, Kongsberg: Modem embed description." (n.d.). [Online]. Available: https://www.kongsberg.com/globalassets/maritime/km-products/product-documents/cnode-modem-embed

[58] S. Sendra, J. Lloret, J. M. Jimenez, and L. Parra, "Underwater acoustic modems," *IEEE Sensors*, vol. 16, no. 11, pp. 4063–4071, Jun. 2016.

[59] Woods Hole Oceanographic Institution, "Applied ocean physics & engineering d.: WHOI micromodem homepage." (n.d.). [Online]. Available: https://acomms.whoi.edu/micro-modem/

[60] P. Hoeher, S. Kaiser, and P. Robertson, "Two-dimensional pilot-symbol-aided channel estimation by Wiener filtering," in *1997 IEEE Int. Conf. Acoust., Speech, Signal Process.*, Munich, Germany, 1997, pp. 1845–1848.

[61] "Model T204 datasheet." (n.d.). [Online]. Available: https://www.neptune-sonar.co.uk/downloads/758580c7-b062-4ddc-9a51-dfcdc9b983b8/T204.pdf

[62] M. Hott, J. M. Placzek, and P. A. Hoeher, "Multi-resonant frequency shift keying: A novel and efficient modulation scheme for magnetic communication," *IEEE Access*, vol. 9, pp. 129431–129442, 2021.

[63] M. Hott, J. M. Placzek, and P. A. Hoeher, "Self-driven high-Q on-off keying: An efficient modulation scheme for magnetic (underwater) communication," in *2022 IEEE Int. Conf. ICT Convergence*, Jeju Island, South Korea, Oct. 2022, pp. 40–44.

[64] M. Hott, J. M. Placzek, and P. A. Hoeher, "Single-frequency-driven multi-resonant FSK: An easy-to-operate wideband modulation scheme for magnetic (underwater) communication," in *2022 IEEE Int. Conf. ICT Convergence*, Jeju Island, South Korea, Oct. 2022, pp. 354–356.
[65] P. A. Hoeher, *Visible Light Communications: Theoretical and Practical Foundations*. Munich, Germany: Carl Hanser, 2019.
[66] C. D. Mobley, *Light and Water*. New York, NY, USA: Academic, 1994.
[67] M. G. Solonenko and C. D. Mobley, "Inherent optical properties of Jerlov water types," *Appl. Opt.*, vol. 54, no. 17, pp. 5392–5401, Jan. 2015.
[68] M. Hott, A. Harlakin, and P. A. Hoeher, "Hybrid communication and localization underwater network nodes based on magnetic induction and visible light for AUV support," in *2020 Int. Conf. Inf. Commun. Technol. Convergence*, Sydney, Australia, Aug. 2020, pp. 66–68.
[69] J. A. Simpson, B. L. Hughes, and J. F. Muth, "Smart transmitters and receivers for underwater free-space optical communication," *IEEE J. Sel. Areas Commun.*, vol. 30, no. 5, pp. 964–974, Jun. 2012.
[70] T. Cimiega and S. Badri-Hoeher, "A cooperative sensor-based navigational concept for heterogeneous AUV swarms," in *2021 IEEE/MTS OCEANS*, San Diego-Porto, Portugal, 2021, pp. 1–10.
[71] International Maritime Organization, *IAMSAR Manual Volume III: Mobile Facilities*. London, U.K.: ICAO, 2022.
[72] M. Held, "FIST: Fast industrial-strength triangulation of polygons," *Algorithmica*, vol. 30, pp. 563–596, 2001.
[73] G. A. Croes, "A method for solving traveling-salesman problems," *Operations Res.*, vol. 6, no. 6, pp. 791–812, 1958.
[74] C. Isokeit, A. Osiik, U. Behrje, and E. Maehle, "Efficient complete coverage path planning for collaborative survey tasks by AUVs," in *Proc. IEEE/MTS OCEANS*, Chennai, India, 2022, pp. 1–10.
[75] K. He, G. Gkioxari, P. Dollár, and R. Girshick, "Mask R-CNN," in *2017 IEEE Int. Conf. Comput. Vis.*, 2017, pp. 2961–2969.
[76] M. Horvat, L. Jelečević, and G. Gledec, "A comparative study of YOLOv5 models performance for image classification," in *Proc. 33rd Central Eur. Conf. Inf. Intell. Syst.*, Dec. 2022, pp. 349–356.
[77] T. Cimiega, L. Boenecke, and S. Badri-Hoeher, "Overview and practical evaluation of sonar-based collision avoidance approaches for AUVs," in *2022 IEEE/MTS OCEANS*, Hampton Roads, VA, USA, 2022, pp. 1–9.

Sabah Badri-Hoeher received the master's degree in physics from the University of Casablanca, Casablanca, Morocco, in 1991, the Dipl.-Ing. (M.Sc.) degree in electrical engineering from the University of Paderborn, Paderborn, Germany, in 1996, and the Dr.-Ing. (Ph.D.) degree in electrical engineering from the University of Erlangen-Nuremberg, Erlangen, Germany, in 2001.

She has been several years with the Fraunhofer Institute of Integrated Circuits in Erlangen, and Kiel University, Kiel, Germany. Since 2009, she has been a Full Professor with the Faculty of Computer Sciences and Electrical Engineering, University of Applied Sciences, Kiel. Her research interests include the general area of signal processing and communication techniques with focus on underwater applications.

Thomas Wilts received the M.Sc. degree in electrical engineering and information technology from CAU, Kiel, Germany, in 2017. He is currently working toward the Ph.D. degree in sonar navigation for autonomous underwater vehicles with the Kiel University of Applied Sciences (UAS), Kiel.

Since 2019, he has been a Research Assistant with UAS. His research interests include sonar data processing, artificial intelligence for autonomous underwater vehicles, and sonar mapping.

Lukas Schaefer, photograph and biography not available at the time of publication.

Jonni Westphalen received the bachelor's degree in computer science from the Kiel University of Applied Sciences, Kiel, Germany, in 2024.

He is working as a Software Developer in the field of naval communication.

Julian Winkler received the master's degree in electrical engineering from the Kiel University of Applied Sciences, Kiel, Germany, in 2022, where he is currently working toward the Ph.D. degree in underwater communication and localization techniques with the Signal Processing Group.

His research interests include underwater localization, navigation, and communication by means of acoustical signals.

Cedric Isokeit received the M.S. degree in underwater robotic swarms from the University of Luebeck, in Germany, in 2016.

He was a Research Associate with the Institute of Computer Engineering, University of Luebeck, Luebeck, Germany. He played a key role in the development of the MONSUN autonomous underwater vehicle (AUV), designed for environmental monitoring and inspection tasks. With the MONSUN AUVs, he participated in the Expedition Clockwork Ocean project, measuring submesoscale eddies. Currently, he works with the industry, developing telematics solutions for fleet management systems. His research interests include development of AUVs as well as mission planning and navigation of robotic swarms.

Andrej Harlakin received the M.Sc. degree in electrical engineering and business administration in 2019 from Kiel University, Kiel, Germany, where he is currently working toward the Ph.D. degree in visible light positioning and communication with the Faculty of Engineering.

Since 2019, he has been a Research and Teaching Assistant with the Chair of Information and Coding Theory, Kiel University. His current research interests include (underwater) visible light positioning and communication, and radar signal processing.

Maurice Hott received the M.Sc. degree in electrical engineering in 2017 from the Institute of Electrical Engineering and Information Technology, Kiel University, Kiel, Germany, where he is currently working toward the Dr.Ing. (Ph.D.) degree in electrical engineering with the Chair of Information and Coding Theory.

Between 2017 and 2022, he has been working as a Research Assistant with the Chair of Information and Coding Theory. His research interests include digital communication for sensor networks and mobile vehicles exploiting modulated magnetic fields in harsh environments.

Julius Maximilian Placzek received the M.Sc. degree in electrical engineering in 2019 from the Institute of Electrical Engineering and Information Technology, Kiel University, Kiel, Germany, where he is currently working toward the Dr.-Ing. (Ph.D.) degree in electrical engineering with the Chair of Power Electronics.

In his bachelor and master theses, he developed and investigated systems for simultaneous wireless information and power transfer with a focus on harsh environments, such as water. His research interests include control of inductive power transfer, battery charging, and talkative power–systems using power flow to communicate information.

Stefan Marx received the graduation degree in physics from the Kiel University, Kiel, Germany,in 1992.

From 1992 to 1993, he worked with the Institute of Applied Physics in the area of Deep-Sea Ocean Engineering. Between 1993 and 1999, he has been the Head of Offshore Sensor Systems, HZG/GKSS Research Center. From 1999 and 2006, he was the Kiel site Manager of 4H-JENA engineering GmbH. In 2006, he cofounded Contros Systems and Solutions GmbH. Finally, in 2010 he founded SubCtech GmbH in Kiel, serving as the CEO. He is an Expert for marine technology and offshore technologies.

Mr. Marx was the recipient of the numerous awards.

Martin Volz, photograph and biography not available at the time of publication.

Erik Maehle (Member, IEEE) received the diploma and doctoral degree in computer science from the University of Erlangen-Nuremberg, Erlangen, Germany, in 1977 and 1982, respectively.

After subsequent positions as a Postdoc with the IBM Zurich Research Laboratory, Rusch-likon, Switzerland, and the University of Erlangen-Nuremberg, he became a Professor with the University of Augsburg, Augsburg, Germany, in 1987 and University of Paderborn, Paderborn, Germany, in 1989. From 1994 to 2017, he was the Director of the Institute of Computer Engineering, University of Luebeck, Luebeck, Germany, and subsequently became a Senior Professor there until 2024. His research interests include mobile robotics, in particular underwater robots, parallel and fault-tolerant computing as well as reconfigurable and organic computing.

Peter Adam Hoeher (Fellow, IEEE) received the Dipl. Ing. degree in electrical engineering from RWTH Aachen University, Aachen, Germany, in 1986, and the Dr. Ing. degree in electrical engineering from the University of Kaiserslautern, Kaiserslautern, Germany, in 1990.

From 1986 to 1998, he was with the German Aerospace Center (DLR), Oberpfaffenhofen, Germany. From 1991 to 1992, he was on leave at AT&T Bell Laboratories, Murray Hill, NJ, USA. Since 1998, he has been a Full Professor of electrical and information engineering with Kiel University, Kiel, Germany. His research interests include the general area of wireless communications and applied information theory.